Control methods for vibration reduction in an underactuated nonlinear beam system

Tackenberg, P.G.H.

Award date:
1997

Control methods for vibration reduction in an underactuated nonlinear beam system

P.G.H. Tackenberg
WFW 97.046

P.G.H. Tackenberg
coaches: M.F. Heertjes and M.J.G. van de Molengraft
Master Thesis
Faculty of Mechanical Engineering
Eindhoven University of Technology
July 1997

Summary

This report presents three control methods to realize vibration reduction for a harmonically excited nonlinear beam system. This system consists of a beam with a one-sided spring attached to the middle, which is harmonically excited in the middle. At the used excitation frequency this system has a stable solution with high vibration amplitude and an unstable solution with low vibration amplitude. The goal is to force the beam system into the unstable solution. The model of the nonlinear beam system has 3-degrees of freedom (DOFs) and one input. The system is a so-called underactuated system, because it has less inputs than DOFs.

The control methods that are compared in this report are: *Partial Feedback Linearization* (PFL), *Computed Desired Computed Torque Control* (CDCTC), and *Computed Reference Computed Torque Control* (CRCTC). These methods make it possible to control the passive DOFs besides the active DOFs, leaving much more freedom in choosing the controlled DOFs. The main difference between PFL and CDCTC/ CRCTC is the usage of a desired/ reference trajectories by CDCTC/ CRCTC enabling feedback of the uncontrolled DOFs along the feedback of the controlled DOFs. The feedback of the error of the uncontrolled DOFs results in an extra contribution to the input that influences the controlled system behavior. Beforehand, it was expected that the extra input contribution could be used to improve the performance in realizing vibration reduction for the nonlinear beam system. It turned out, however, to be impossible to use the extra input contribution to improve the performance due to the lack of understanding its possibilities

A cart-pole system is controlled with the three methods to gain insight in the use of the methods. By investigating the zero dynamics of the closed loop system with PFL, information is obtained about the behavior of the uncontrolled DOFs when the controlled DOF has reached its desired trajectory. The best performance for the cart-pole that is found is realized with CRCTC. Despite the fact that the performance can be improved with the extra input contribution, its influence remains unpredictable, because a change of the initial conditions can change the influence of the extra input contribution. The relation between the influence of the extra input contribution, and the control gains and initial conditions remains unclear.

The nonlinear beam system is controlled to realize vibration reduction. By proving that the unstable harmonic solution is a globally asymptotic stable solution of the zero dynamics of the closed loop system, it can be guaranteed that all DOFs reach that solution. The best performance is realized with PFL. This is caused by the fact that the feedback of the errors with CDCTC and CRCTC is partly determined by the system matrices. Furthermore, no set of gains for CDCTC and CRCTC is found that resulted in an extra input contribution that improved the system behavior.

The main conclusion of this report is that the system behavior can be influenced with the extra input contribution created by CDCTC and CRCTC in comparison with PFL. However, the lack of understanding into the relation between the extra input contribution and the controlled system behavior makes the influence of this force unpredictable.

Contents

Summary i

Notation iii

1 Introduction 1

2 Control Methods for Underactuated Systems 3
- 2.1 Introduction . . . 3
- 2.2 Partial Feedback Linearization (PFL) . . . 4
- 2.3 Computed Desired Computed Torque Control (CDCTC) . . . 7
- 2.4 Computed Reference Computed Torque Control (CRCTC) . . . 9
- 2.5 Discussion . . . 10

3 Cart-Pole System; a Case Study 12
- 3.1 Introduction . . . 12
- 3.2 Model of a Cart-Pole System . . . 13
- 3.3 Simulations with Partial Feedback Linearization . . . 13
- 3.4 Simulations with Computed Desired Computed Torque Control . . . 18
- 3.5 Simulations with Computed Reference Computed Torque Control . . . 21
- 3.6 Discussion . . . 25

4 Beam with One-Sided Spring 27
- 4.1 Introduction . . . 27
- 4.2 Model of the Beam with One-Sided Spring . . . 27
- 4.3 Simulation with Partial Feedback Linearization . . . 29
- 4.4 Simulation with Computed Desired Computed Torque Control . . . 32
- 4.5 Simulation with Computed Reference Computed Torque Control . . . 36
- 4.6 Discussion . . . 38

5 Conclusions and Recommendations 40
- 5.1 Conclusions . . . 40
- 5.2 Recommendations . . . 41

Bibliography 42

A Model matrices 43

Notation

Symbols

a	column
a_i	i-th element of a
$\dot{a}$	first time derivation of a
$\ddot{a}$	second time derivation of a
A	matrix
$A_{i,j}$	ij-th element of A where i indicates the row and j the column
$A_{i:j,k:l}$	sub-matrix of A with from row i through j the element of column k through l
$A_{i\ j,k\ l}$	sub-matrix of A with from row i and j the element of column k and l
A^{-1}	inverse of A
A^T	transpose of A

Abbreviations

CDCTC	Computed Desired Computed Torque Control
CRCTC	Computed Reference Computed Torque Control
CTC	Computed Torque Control
DOF(s)	Degree(s) Of Freedom
PFL	Partial Feedback Linearization
SCTC	Sliding Computed Torque Control

Chapter 1

Introduction

The subject of this study is the vibration reduction of harmonically excited nonlinear systems. Examples of such systems are: suspension bridges excited by the wind, or ships at quay sides excited by the water. A characteristic of harmonically excited systems is the occurrence of vibrations with large amplitudes, which are generally undesired since they cause wear and are responsible for high levels of noise. To reduce these vibrations, investigation in the steady state behavior of harmonically excited systems with local nonlinearities has been done [2]. The steady-state response of such system exhibits two or more coexisting solutions of the system for certain frequency ranges. When the system is forced into the natural solution with lowest vibration amplitude the wear and noise levels will drop. The advantage of forcing the system into a natural solution is that, when the system reaches this solution, the control force will become zero; this only holds under perfect modeling conditions, i.e. no disturbances, model errors etc.

An example of a harmonically excited nonlinear system is the nonlinear beam system that is used in earlier studies to verify theoretical results. This system consists of a beam with a one-sided spring attached to the middle. The beam is harmonically excited in the middle by means of a rotating mass unbalance. The steady state response consists of at least two coexisting solutions namely, a stable $\frac{1}{2}$ subharmonic solution of high amplitude and an unstable harmonic solution of low amplitude. Without control the system can vibrate in the stable $\frac{1}{2}$ subharmonic solution. The control objective is to force the system into the unstable harmonic solution. In this way, wear and noise levels will drop, while the control effort remains small due to the fact that a natural solution of the system is used.

The nonlinear beam system has, in principle, an infinite number of degrees of freedom (DOFs). In practice, when a model of the beam system is used, the number of DOFs will be reduced, but in general there will still be more DOFs than inputs. Systems that have more DOFs than inputs are called underactuated systems. Other examples of underactuated systems are robots with flexible joints and links, space robots and mobile robots. The DOFs of an underactuated system can be divided in two parts: the active DOFs, which can be influenced directly by the inputs, and the passive DOFs. The beam system, used in this study, exhibits only one input, applied at a quarter of the beam while the model used is based on 3-DOFs.

Vibration reduction for this beam system has been accomplished earlier with Computed Torque Control (CTC) and Sliding Computed Torque Control (SCTC), in simulations by Kant [5] and experimentally by Heertjes et al. [3]. Both control techniques are developed to control nonlinear systems and are discussed by Slotine and Li [7]. With (S)CTC it is only possible to control the active DOFs. So the active DOFs can be forced into the unstable harmonic solution. These control methods, however, do not take into account the passive DOFs. So we want to use control methods, to reduce the vibration of the beam, which guarantee that all DOFs are forced into the unstable harmonic solution. Besides this we want to see if it is

possible to control the passive DOFs instead of the active DOFs in order to improve control performance for the total system.

Two control methods for underactuated systems are considered, namely: *Partial Feedback Linearization* (PFL, Spong [8]) and *Computed Reference Computed Torque Control* (CRCTC, Lammerts [4]). Both methods make it possible to 'say' something about the behavior of the uncontrolled DOFs. They are also capable of controlling passive DOFs through the active DOFs. In this study PFL and CRCTC are used to accomplish vibration reduction for the nonlinear beam system. CRCTC has been used earlier by Kant [5] who investigated the method in comparison with CTC. This study, however, omits a proper treatment of CRCTC. There are also doubts about the way that CRCTC has been compared to CTC, which influences the conclusions. Therefore CRCTC is investigated again. The goals of this study can be summarized as: *gain more understanding of the performance of both methods within our class of underactuated systems.*

During the research it turned out that the two methods PFL and CRCTC could not be compared with each other in a fair way. This would result in the fact that no conclusions could be drawn regarding the basic difference between the two methods. To prevent this, Computed Desired Computed Torque Control (CDCTC) by Lammerts [4] has been used to control the beam system. This method is basically the same as CRCTC but can be compared with PFL in a fair way. The introduction of CDCTC is also used for gaining insight into the basics of CRCTC. Furthermore, it was expected that CRCTC and CDCTC, in contradiction to PFL, were able to influence the uncontrolled DOFs and so to perform better than PFL. The outcome, however, of this study did not support this expectation, because the extra input contribution created with CRCTC and CDCTC, could no be related clearly to the gains, the initial condition, and the system dynamics which made the performance unpredictable.

This report is set up as follows. In Chapter 2 the theoretical foundations of PFL, CDCTC and CRCTC will be discussed. Chapter 3 will present a case study of a cart-pole, to gain more insight in the applicability of the control methods. Simulation results of the nonlinear beam system with PFL, CDCTC and CRCTC will be presented in Chapter 4, followed by a discussion of the differences between the control methods. Finally in Chapter 5 conclusions and suggestions for further research will be given.

Chapter 2

Control Methods for Underactuated Systems

2.1 Introduction

Before turning our attention to the control methods, we start with a description of underactuated systems. Underactuated systems are systems which possess fewer actuators than DOFs. A simple example of an underactuated system is the mass-damper-spring system in Figure 2.1. This system has two DOFs, i.e. the positions x_1 and x_2 of the masses m_1 and m_2. Furthermore, this system has one input u working on mass m_1. Underactuation implies that only one of the masses can be controlled in a direct way. Another example of an underactuated systems is a lightweight robot, where the flexibility in links and/or joints cannot be ignored. The nonlinear beam used in this study is a particular example of an underactuated system.

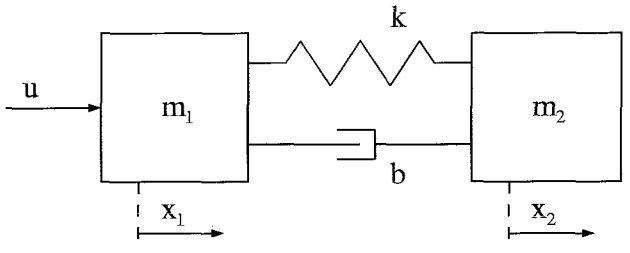

Figure 2.1: A mass-damper-spring system with one input.

The DOFs $q \in \Re^n$ of an underactuated system can be divided in two sets: a set of actuated or active DOFs $q_a \in \Re^l$ and a set of unactuated or passive DOFs $q_p \in \Re^m$. The active DOFs represent that part of the DOFs that can be directly influenced by the inputs. In the example of the mass-damper-spring system (Figure 2.1), the active DOF is represented by x_1 and the passive DOF is represented by x_2. Besides this division, the DOFs can be divided in controlled DOFs q_c (as many as there are inputs), and uncontrolled DOFs q_u. We want the choice of q_c to be independent from the system configuration. Using, however, a specific control method, restricts the possibilities for the choice for q_c. When for example CTC (Slotine and Li [7]) is used to control the mass-damper-spring system, only the active DOF x_1 can be chosen as q_c.

The control methods PFL (Spong [8]), CDCTC and CRCTC (Lammerts [4]), are especially developed to control underactuated system. The advantages of these methods compared with (S)CTC are the fol-

lowing. Firstly, it is possible to 'say' something about the behavior of the uncontrolled DOFs, without explicit simulation of the system behavior. Secondly, it is possible to control passive DOFs instead of active DOFs. This freedom, however, is restricted, to some extent, by the possibilities of the used method.

In case of vibration reduction of a harmonically excited beam system, we want to accomplish a reduction for all DOFs and not only for the controlled DOFs. This is where the difference between PFL and CDCTC/ CRCTC appears. In earlier studies a coupling between the controlled DOFs and the uncontrolled DOFs has been noticed; the behavior of the controlled DOFs influences the behavior of the uncontrolled DOFs. It is our intention to influence the behavior of the uncontrolled DOFs by using the controlled DOFs. At the cost of decreasing performance for the controlled DOFs, the total performance of the system is expected to improve. Furthermore, it is expected that this is directly possible with CDCTC and CRCTC, due to the fact that CDCTC and CRCTC use an on-line calculated desired trajectory for the uncontrolled DOFs which means that the error feedback for all DOFs becomes possible.

The outline of this chapter is as follows: a description of PFL will be given together with restrictions on the choice of q_c followed by CDCTC and CRCTC. This chapter will conclude with a comparison between the three control methods.

2.2 Partial Feedback Linearization (PFL)

Feedback linearization (Slotine and Li [7]) is a nonlinear control technique that guarantees desired tracking behavior for the whole state, when applied to a fully actuated system, satisfying the proper conditions. If the system is not fully actuated, only a part of the state can be controlled using feedback linearization. This case is often referred to as PFL. PFL has been used by Spong [8] to control an acrobot; a robot with two joints and only one actuator.

Before using PFL for control, two preparing steps have to be carried out. The first step deals with the choice of the controlled DOFs q_c. When the controlled DOFs are equal to the active DOFs ($q_c = q_a$) we have the so-called collocated case. In that case PFL is the same as CTC used by Kant [5] . We will, however, exploit the knowledge of the zero dynamics in order to investigate the behavior of the passive DOFs q_p beforehand. Another possible choice for q_c is $q_c = q_p$, which is often referred to as the non-collocated case. This choice is only possible when the passive DOFs are inertially coupled with the active DOFs and the number of DOFs in q_p is equal to or less than the number of inputs; coupling is needed to pass energy from the inputs to q_p. Looking at the earlier given example of the mass-damper-spring system, there is no inertial coupling (the mass matrix is diagonal) between the two DOFs and so it is not possible to use PFL to control x_2. The case where an arbitrary selection of the active and passive DOFs is chosen as the controlled DOFs, is not investigated in this study. The second step is to write the underactuated system in a general form:

$$M_{aa}\,\ddot{q}_a + M_{ap}\,\ddot{q}_p + h_a + f_a = u, \tag{2.1}$$

$$M_{pa}\,\ddot{q}_a + M_{pp}\,\ddot{q}_p + h_p + f_p = 0. \tag{2.2}$$

With M_{aa}, M_{ap}, M_{pa} and M_{pp} representing the sub-matrices of the inertia matrix $M = M(q)$, $h_a = h_a(\dot{q}, q)$ and $h_p = h_p(\dot{q}, q)$ represent the Coriolis and centrifugal terms, and u are the inputs. $f_a = f_a(\dot{q}, q, t)$ and $f_p = f_p(\dot{q}, q, t)$ represent forces like gravity, damping, spring, and external forces.

$$M = \begin{bmatrix} M_{aa} & M_{ap} \\ M_{pa} & M_{pp} \end{bmatrix}.$$

The collocated case

In the collocated case the controlled DOFs are equal to the active DOFs ($q_c = q_a$). The system is partially feedback linearized with respect to q_a. To make this possible, equation (2.2) is used to substitute $\ddot{q}_p$ in Eq. (2.1). For this purpose, Eq. (2.2) is solved for $\ddot{q}_p$, resulting in:

$$\ddot{q}_p = -M_{pp}^{-1}\,(M_{pa}\,\ddot{q}_a + h_p + f_p), \tag{2.3}$$

which requires M_{pp} to be invertible. Substituting Eq. (2.3) in Eq. (2.1) results in:

$$(M_{aa} - M_{ap}\,M_{pp}^{-1}\,M_{pa})\,\ddot{q}_a + h_a - M_{ap}\,M_{pp}^{-1}\,h_p + f_a - M_{ap}\,M_{pp}^{-1}\,f_p = u. \tag{2.4}$$

A proper choice for the input u is:

$$u = (M_{aa} - M_{ap}\,M_{pp}^{-1}\,M_{pa})\,v + h_a - M_{ap}\,M_{pp}^{-1}\,h_p + f_a - M_{ap}\,M_{pp}^{-1}\,f_p, \tag{2.5}$$

where v is an additional control input yet to be defined. The system equations (2.1) and (2.2) are rewritten using u as defined in Eq. (2.5), which results in:

$$\ddot{q}_a = v, \tag{2.6}$$

$$M_{pa}\,v + M_{pp}\,\ddot{q}_p + h_p + f_p = 0. \tag{2.7}$$

The system is partially feedback linearized by the choice of u, resulting in a linear set of double integrators, Eq. (2.6) with a new control input v, and a passive part, also called the internal dynamics described by Eq. (2.7), which will be nonlinear in general. v can be chosen such that q_a will asymptotically tend to the desired trajectory q_{a_d}. A possible choice for v is:

$$v = \ddot{q}_{a_d} + k_d\,(\dot{q}_{a_d} - \dot{q}_a) + k_p\,(q_{a_d} - q_a), \tag{2.8}$$

where k_p and k_d are $l \times l$ gain matrices. Eq. (2.8) combined with Eq. (2.6) gives an asymptotically stable differential equation leading to the desired trajectory for the controlled DOFs q_c.

The remaining question is how the uncontrolled DOFs in the collocated case, q_p, behave. This can be investigated by looking at the internal dynamics of the system, represented by Eq. (2.7). From Eq. (2.7) follows that the internal dynamics depends on the input v, and is therefore difficult to interpret. To make this easier the following state variables are defined: $z_1 = q_{a_d} - q_a$, $z_2 = \dot{q}_{a_d} - \dot{q}_a$, $\eta_1 = q_p$ and $\eta_2 = \dot{q}_p$. The closed loop system Eq. (2.6), Eq. (2.7) and Eq. (2.8) can now be written as:

$$\dot{z} = A\,z, \tag{2.9}$$

$$\dot{\eta} = w(\eta, z, t), \tag{2.10}$$

where z, η, A and $w(\eta, z, t)$ are given by:

$$z = \begin{bmatrix} z_1 \\ z_2 \end{bmatrix}, \quad \eta = \begin{bmatrix} \eta_1 \\ \eta_2 \end{bmatrix}, \quad A = \begin{bmatrix} 0 & 1 \\ -k_p & -k_d \end{bmatrix},$$

$$w = \begin{bmatrix} \eta_2 \\ -M_{pp}^{-1}\,(h_p + f_p + M_{pa}\,(\ddot{q}_{a_d} + k_d\,z_2 + k_p\,z_1)) \end{bmatrix}.$$

z is the controlled variable in this new system description. The surface $z = 0$ in state space defines an invariant manifold for the system; the manifold is called invariant because at the manifold the state remains at the manifold as time increases. On this manifold, the behavior of the system dynamics is described by:

$$\dot{\eta} = w(\eta, 0, t). \tag{2.11}$$

Spong [8] calls this the zero dynamics of the system. But by Slotine and Li [7, Chapter 6.1] the zero dynamics is defined as: *the internal dynamics of the system when the system output is kept zero by the input.* This means that Spong redefines the output as $y = z$ instead of $y = q_c$. With Eq. (2.11) we investigate the zero dynamics with respect to the new defined output z, the zero dynamics of the closed loop system.

The zero dynamics of the closed loop system Eq. (2.11) is independent of the gain matrices k_p and k_d. These gains, however, together with the initial condition, completely determine the position where the system enters the zero dynamics of the closed loop system and, thus, which particular trajectories the uncontrolled DOFs follow.

The non-collocated case

In the non-collocated case the controlled DOFs are equal to the passive DOFs ($q_c = q_p$). As mentioned earlier, this is only possible when there is inertial coupling between q_a and q_p i.e. the inverse of M_{pa} exists. This can be understood physically by the fact that this coupling is needed to pass energy from the actuated DOFs to the unactuated DOFs. (However, energy can also be passed throughout the system using springs and dampers. This will be the basis for the derivation of CDCTC in the next subsection.) The system is locally inertially coupled if:

$$\text{rank}(M_{pa}(q)) = m \quad \text{for all} \quad q \in \mathcal{B},$$

where $\mathcal{B}$ is a neighborhood of the origin. When this coupling is global this means that its holds for all $q \in \Re^n$. There is another restriction for the non-collocated case: the number of passive DOFs, m has to be less than or equal to the number of inputs l ($m \leq l$).

The system equations (2.1) and (2.2) can now be partially feedback linearized with respect to q_p. Eq. (2.2) is used to substitute q_a in Eq. (2.1) (instead of q_p as in the collocated case). Solving Eq. (2.2) for q_a leads to:

$$\ddot{q}_a = -M_{pa}^{-1}\,(M_{pp}\,\ddot{q}_p + h_p + f_p). \tag{2.12}$$

The next step, substituting Eq. (2.12) in Eq. (2.1), results in:

$$(M_{ap} - M_{aa}\,M_{pa}^{-1}\,M_{pp})\,\ddot{q}_p + h_a - M_{aa}\,M_{pa}^{-1}\,h_p + f_a - M_{aa}\,M_{pa}^{-1}\,f_p = u. \tag{2.13}$$

A proper choice for u is:

$$u = (M_{ap} - M_{aa}\,M_{pa}^{-1}\,M_{pp})\,v + h_a - M_{aa}\,M_{pa}^{-1}\,h_p + f_a - M_{aa}\,M_{pa}^{-1}\,f_p, \tag{2.14}$$

where v is an additional control input. As in the collocated case, but now with respect to the passive DOFs, the system equations can be written as:

$$\ddot{q}_p = v, \tag{2.15}$$

$$M_{pa}\,\ddot{q}_a + M_{pp}\,v + h_p + f_p = 0. \tag{2.16}$$

The goal is letting q_p follow a desired trajectory q_{p_d}. For this purpose the structure of v is chosen similar to the collocated case Eq. (2.8), leading to:

$$v = \ddot{q}_{p_d} + k_d\,(\dot{q}_{p_d} - \dot{q}_p) + k_p\,(q_{p_d} - q_p), \tag{2.17}$$

where k_p and k_d are $l \times l$ gain matrices.

The behavior of the uncontrolled DOFs (in this case q_a) as again determined by the internal dynamics. To make the investigation of the internal dynamics easier, we again (as in the collocated case) look at the closed loop system. Therefore the following state variables are defined: $z_1 = q_{p_d} - q_p$, $z_2 = \dot{q}_{p_d} - \dot{q}_p$, $\eta_1 = q_a$ and $\eta_2 = \dot{q}_a$. The closed loop system can now be written in the same form as in the collocated case, resulting in:

$$\dot{z} = A\,z, \tag{2.18}$$

$$\dot{\eta} = w(\eta, z, t). \tag{2.19}$$

The zero dynamics with respect to the output z can be given by:

$$\dot{\eta} = w(\eta, 0, t). \tag{2.20}$$

As in the collocated case Eq. (2.20) will be referred to as the zero dynamics of the closed loop system.

2.3 Computed Desired Computed Torque Control (CDCTC)

The second control technique used in this study is CDCTC. For a complete survey on CDCTC the reader is referred to Lammerts [4]. CDCTC is developed for the control of flexible manipulators and is used in this study to obtain insight in the actual difference between CRCTC (which will be explained in Subsection 2.4) and PFL. This is due to the possibility to compare CDCTC in a fair way with PFL (which we shall see is not the case for CRCTC). The main difference between CDCTC and PFL which we shall discuss is the possibility of using errors of the uncontrolled DOFs for feedback. Besides this the introduction of CDCTC will explain the structure of CRCTC in a more plain manner.

Using the coupling between the passive and active DOFs, the idea of CDCTC is to control an unactuated DOF, by translating the desired trajectory for this DOF to a pseudo desired trajectory for the actuated DOF. Next, an input is computed which assures that the actuated DOF follows the pseudo desired trajectory, and so makes sure that the unactuated DOF follows the desired trajectory. The trajectory for the actuated DOF is computed by solving the differential equation of the passive part. To understand this idea we look again at the earlier used example of the mass-damper-spring system (Figure 2.1) with the following system equations:

$$m_1\ddot{x}_1 + b(\dot{x}_1 - \dot{x}_2) + k(x_1 - x_2) = u, \tag{2.21}$$

$$m_2\ddot{x}_2 + b(\dot{x}_1 - \dot{x}_2) + k(x_1 - x_2) = 0. \tag{2.22}$$

As mentioned earlier x_1 represents the active DOF and x_2 represents the passive DOF. To control x_2 (which is not possible with PFL because there is no inertial coupling) the desired trajectory for x_2 has to be translated to a pseudo desired trajectory for x_1. This is done by using Eq. (2.22) where the desired trajectory x_{2_d} is substituted:

$$m_2\ddot{x}_1 + b\dot{x}_1 + kx_1 = b\dot{x}_{2_d} + kx_{2_d}. \tag{2.23}$$

Solving Eq. (2.23) leads to a pseudo desired trajectory for x_1, namely x_{1_d}. Next an input is chosen in such a way that x_1 tracks the pseudo desired trajectory, or:

$$u = m_1 v + b(\dot{x}_1 - \dot{x}_2) + k(x_1 - x_2), \tag{2.24}$$

with the new input v chosen as:

$$v = \ddot{x}_{1_d} + k_d(\dot{x}_1 - \dot{x}_{1_d}) + k_p(x_1 - x_{1_d}). \tag{2.25}$$

The desired result is only obtained when the initial state of the system is equal to the desired state at t_0 and when there are no disturbances working on the system.

In general, this idea has to be adapted, such that the passive DOFs follow their desired trajectories when the initial condition are not the same as the desired ones, and in case of disturbances. This addition of robustness results in CDCTC as presented below.

To present CDCTC, the following system description is used:

$$M\ddot{q} + C\dot{q} + B\dot{q} + Kq + f_n = H\,u, \tag{2.26}$$

where $M = M(q)$ is the symmetric, positive definite inertia matrix, $C = C(\dot{q}, q)$ is the matrix which accounts for the Coriolis and centrifugal terms, B is the symmetric (semi-) positive definite damping matrix, K is the symmetric (semi-) positive definite stiffness matrix, and $f_n = f_n(\dot{q}, q, t)$ represents forces like gravity, nonlinear damping, nonlinear stiffness, and external forces. H is called a distribution matrix, where rank$(H) = l$ with l the number of inputs.

The DOFs are divided in two parts: the controlled DOFs, $q_c \in \Re^l$, where l is the number of inputs and the uncontrolled DOFs, $q_u \in \Re^m$. Both sets can exhibit active and passive DOFs. This division can be written as:

$$q = L_c\,q_c + L_u\,q_u, \tag{2.27}$$

where L_c and L_u are permutation matrices. The only restriction on the choice of this division is that is has to be possible to compute a bounded desired trajectory for q_u.

The control goal can be formulated as to determine a bounded input u so that the DOFs q_c track their desired trajectories asymptotically, under the strict condition that the DOFs q_u remain bounded. When the tracking error is defined as: $e_c = q_{c_d} - q_c$, the control goal can be specified as follows: determine a bounded u such that e_c and its derivative $\dot{e}_c$ converge to zero asymptotically, while q_u and $\dot{q}_u$ remain bounded.

For now we assume that it is possible to compute a bounded desired trajectory for q_u (q_{u_d}), as with the pseudo desired trajectory in the example of the mass-damper-spring system. How q_{u_d} is computed will be shown in a later stage. It is now possible to present the desired trajectories as follows:

$$q_d = L_c\,q_{c_d} + L_u\,q_{u_d}, \tag{2.28}$$

$$e = q_d - q = L_c\,e_{c_d} + L_u\,e_{u_d}. \tag{2.29}$$

The control goal is achieved if a bounded input can be found such that $\dot{e} \to 0$ and $e \to 0$ for $t \to \infty$. To realize this Lammerts [4] has chosen Hu as:

$$H\,u = M\ddot{q}_d + C\dot{q}_d + B\dot{q}_d + Kq_d + f_n + K_d\,\dot{e} + K_p\,e, \tag{2.30}$$

where K_d and K_p are positive definite gain matrices. This choice combined with Eq. (2.26) results in the following error equations:

$$M\ddot{e} + (C + B + K_d)\dot{e} + (K + K_p)e = 0. \tag{2.31}$$

With the second method of Lyapunov, it can be shown that $e = 0$ is an asymptotically stable equilibrium point of the error equation (2.31). So with Eq. (2.30) as input of Eq. (2.26) it is guaranteed that q_c will asymptotically converge to q_{c_d}. Furthermore, with the assumption that it is possible to compute a bounded solution for q_{u_d}, it is also guaranteed that q_u remains bounded. The remaining problem is to compute a bounded q_{u_d}. Eq. (2.30) is a set of n equation and there are only l equation necessary to compute l inputs. The idea is to use the remaining m equation to compute q_{u_d}. So Eq. (2.30) is split in two parts. An active part to determine the inputs and a passive part for calculating q_{u_d}. Because the passive part depends on the actual state of the system, it has to be solved on-line. To split Eq. (2.30) into a part to compute u, and a part to compute a bounded q_{u_d}, a new matrix $N \in \Re^{l \times m}$ is introduced such that $N^T H = 0$. With this new matrix N, Eq. (2.30) can be written as:

$$u = (H^T H)^{-1} H^T [M\ddot{q}_d + C\dot{q}_d + B\dot{q}_d + Kq_d + f_n + K_d\dot{e} + K_p e], \tag{2.32}$$

$$0 = N^T [M\ddot{q}_d + C\dot{q}_d + B\dot{q}_d + Kq_d + f_n + K_d\dot{e} + K_p e]. \tag{2.33}$$

Whether it is possible to compute a bounded q_{u_d}, strongly depends on the properties of Eq. (2.33). When Eq. (2.33) is a stable differential equation for q_{u_d}, a bounded desired trajectory can be computed on-line. For the computation of q_{u_d} we also need an initial choice for $\dot{q}_{u_d}(t_0)$ and $q_{u_d}(t_0)$. A possible, and often used, choice is $\dot{q}_{u_d}(t_0) = \dot{q}_u(t_0)$ and $q_{u_d}(t_0) = q_u(t_0)$. The desired trajectory for q_u computed in this way, not only depends on q_{c_d}, but also depends on the actual state of all DOFs, which is caused by the introduction of the feedback of errors of all DOFs. This results in the error equation (2.31) which guarantees the desired trajectory for the controlled DOFs to be globally asymptotically stable. So it is possible to obtain a desired trajectory for q_c (where q_c is an arbitrary choice of q) with CDCTC, if and only if it is possible to compute a bounded desired trajectory for the uncontrolled DOFs.

2.4 Computed Reference Computed Torque Control (CRCTC)

The third and last control technique used in this study is CRCTC [4]. CRCTC is strongly related to CDCTC. It has been used to control several nonlinear flexible manipulators in simulations and experiments. The main difference between CRCTC and CDCTC is the usage of reference trajectories instead of desired trajectories which enables the use of adaptive control. CRCTC has been used earlier by Kant [5] to control the nonlinear beam, however, questions concerning the applicability of the method remained. The influence of the reference trajectories on the control performance remained unknown. Furthermore, there were doubts about the validity of the comparison between CRCTC and CTC.

The idea behind CRCTC is the same as with CDCTC. However, instead of a desired trajectory a reference trajectory is introduced, defined by:

$$\dot{q}_{c_r} = \dot{q}_{c_d} + \Lambda_c e_c, \qquad e_c = q_{c_d} - q_c, \tag{2.34}$$

with Λ_c a positive definite gain matrix. The introduction of the reference trajectory is a notation manipulation which makes the extension to adaptive control possible in order to account for parametric uncertainty. The control goal can now be reformulated with a reference error defined by: $e_{c_r} = q_{c_r} - q_r$. The tracking requirements are guaranteed if $\dot{e}_{c_r} \to 0$ for $t \to \infty$. When q_r is needed, it has to be computed by integrating $\dot{q}_{c_r}$. An initial value for q_{c_r} can be chosen freely, a trivial choice is $q_{c_r}(t_0) = q_c(t_0)$.

The input must also guarantee that q_u and $\dot{q}_u$ remain bounded. Assuming that it is possible to compute a bounded desired trajectory q_{u_d}, a reference trajectory can also be defined for q_u:

$$\dot{q}_{u_r} = \dot{q}_{u_d} + \Lambda_u e_u, \qquad e_{u_d} = q_{u_d} - q_u, \tag{2.35}$$

with positive definite matrix Λ_u and a suitable initial value. A possible choice suggested by Lammerts [4] is $q_{u_r}(t_0) = q_u(t_0)$ and $\dot{q}_{u_r}(t_0) = \dot{q}_u(t_0)$. q_{u_r} will be determined in a same way as q_{u_d} when CDCTC is used. The total reference trajectory and reference error are given as:

$$q_r = L_c\, q_{c_r} + L_u\, q_{u_r}, \tag{2.36}$$

$$e_r = q_r - q = L_c\, e_{c_r} + L_u\, e_{u_r}, \tag{2.37}$$

where $e_{c_r} = q_{c_r} - q_c$ and $e_{u_r} = q_{u_r} - q_u$.

In order to realize the control objectives, Hu is chosen in a similar way as with CDCTC, resulting in:

$$H\,u = M\ddot{q}_r + C\dot{q}_r + B\dot{q}_r + Kq_r + f_n + K_r\,\dot{e}_r, \tag{2.38}$$

where K_r is a positive definite gain matrix. Substitution in Eq. (2.26) results in the following reference error equation:

$$M\ddot{e}_r + (C + B + Kr)\dot{e}_r + Ke_r = 0. \tag{2.39}$$

It is not possible to show with the second method of Lyapunov, that $e_r = 0$ is a stable equilibrium point. This is caused by the fact that K is semi-positive definite. It can be shown, however, that $\dot{e}_r$ becomes zero for $t \to \infty$ and that e_r is bounded. This fact combined with the definition of e_r is enough to guarantee that q_c tends towards q_{c_d} while q_{u_r} remains bounded.

Again the remaining problem is computing q_u. This is done in the same way as with CDCTC. Eq. (2.38) is split into an active and passive part using a matrix $N \in \Re^{l\times m}$. N is chosen such that $N^T H = 0$. The set of equations can be written as:

$$u = (H^T H)^{-1}\, H^T\, [M\ddot{q}_r + C\dot{q}_r + B\dot{q}_r + Kq_r + f_n + K_r\,\dot{e}_r], \tag{2.40}$$

$$0 = N^T [M\ddot{q}_r + C\dot{q}_r + B\dot{q}_r + Kq_r + f_n + K_r\,\dot{e}_r]. \tag{2.41}$$

Whether it is possible to compute a bounded q_{u_r} on-line, depends on the properties of Eq. (2.41).

2.5 Discussion

The three outlined control methods are developed to control underactuated systems. The advantage is that the user is given much more freedom in choosing the controlled DOFs, and the ability to 'say' something about the behavior of the uncontrolled DOFs without using explicit simulation of the system behavior. The three control methods have their own restriction on the choice of controlled DOFs, and the way the behavior of the uncontrolled DOFs is investigated.

The first control method of this chapter was PFL. Using PFL, two cases are distinguished: the collocated case where the active DOFs are controlled, and the non-collocated case, where the passive DOFs are controlled. In the collocated case PFL results in the same behavior as CTC. Control of the passive DOFs is only possible under strict conditions; there has to be inertial coupling. Furthermore, the number of passive

DOFs has to be less than or equal to the number of inputs. The examination of the behavior of uncontrolled DOFs is in both cases the same, and is done with the usage of the zero dynamics of the closed loop system. This gives a reduction in computational effort due to the fact that the order of the zero dynamics is less than the order of the model under investigation.

The second control method of this chapter was CDCTC. This method can exploit not only the inertial coupling (as in case of PFL) but all possible forms of coupling such as coupling created by dampers or springs. The choice of the controlled DOFs with CDCTC is only restricted to the possibility to compute bounded pseudo desired trajectories on-line. These computed pseudo desired trajectories guarantee, together with the chosen input, that the controlled DOFs will track the desired trajectories and that the uncontrolled DOFs remain bounded. It is, however, difficult to interpret the path of these computed pseudo desired trajectories physically. The computed pseudo desired trajectories enable to the possibility to use errors of all DOFs for feedback. It is expected that this improves the performance of CDCTC compared to PFL in for example vibration reduction for the harmonically excited beam system. The computation of the pseudo desired trajectories can certainly become a problem when the differential equations are difficult to solve, which limits the applicability of the hardware.

The last control method of this chapter was CRCTC, that is strongly related to CDCTC. The difference is that instead of the pseudo desired trajectories, reference trajectories are used. The advantage is that this method can be extended to adaptive control. But, it is even harder to interpret the physical meaning of the computed reference trajectories in comparison with the pseudo desired trajectories of CDCTC. The controlled DOFs can be chosen freely as long as it is possible to compute the bounded reference trajectories. The computed reference trajectories guarantee, together with the input, that the uncontrolled DOFs remain bounded. The computation of the reference trajectories put, as the pseudo desired trajectories of CDCTC, high demands on the hardware when the differential equations are difficult to solve.

Chapter 3

Cart-Pole System; a Case Study

3.1 Introduction

To gain more insight in the usability of the three control methods, discussed in the previous chapter, the so called cart-pole system, an underactuated system, is used as an example (see Figure 3.1). The cart-pole system has been used earlier by Slotine and Li ([7]) and Spong ([8]). The advantage of the cart-pole is that it is a nonlinear system of which the behavior can be relatively easy understood. When, for example, the goal is to control the pole from $\phi = 0$ [rad] to $\phi = \frac{\pi}{4}$, it can be imagined, that the cart has to be pulled to the left before pushing it to the right to achieve this desired behavior.

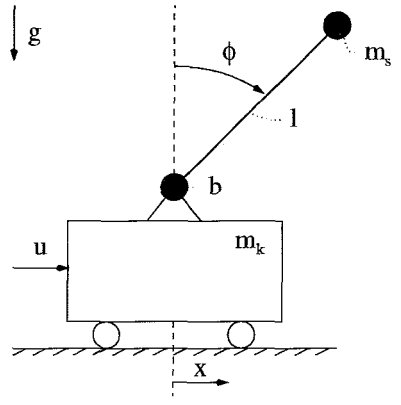

Figure 3.1: The cart-pole system.

The cart-pole system has two DOFs, the position of the cart x and the angle of the pole ϕ. Furthermore, the system has one input u, the driving force on the cart. So the cart-pole has less inputs than DOFs and is therefore an underactuated system. The position of the cart is the DOF that can be influenced directly by the input and is the active DOF q_a. Opposite to this, the angle is the passive DOF q_p. Besides this the DOFs can be divided in a controlled DOF q_c and an uncontrolled DOF q_u. There are two possible choices for this division. The first choice is to control the position of the cart-pole (the active DOF). According to Section 2.3 this is called the collocated case. The second choice is to control the angle of the pole (the passive DOF) and is called the non-collocated case.

In the collocated case a possible control goal can be formulated as: controlling the cart from an arbitrarily start position to a desired position within a pre-defined time interval. The difference between PFL and

CDCTC/ CRCTC, however, appears when requirements are put on the uncontrolled DOFs. Therefore, the control goal used in this study for the cart-pole is: controlling the cart from an arbitrarily start position to a desired position, where the pole is aimed downwards, within a pre-defined time interval. In addition, we want to make this time interval as short as possible. In the non-collocated case, where the angle is controlled, the control goal is defined as: controlling the pole from an arbitrarily start angle to a desired angle within a pre-defined time interval. In this case the control goal is not expanded with requirements for the uncontrolled DOF.

In this chapter, we will first discuss briefly the model of the cart-pole system, followed by simulations with the cart-pole using PFL. Also simulation of the cart-pole system using CDCTC and CRCTC will be presented. These simulations will be followed by a discussion on the three control methods in relation to each other, when controlling the cart-pole.

3.2 Model of a Cart-Pole System

The model of the cart-pole system can be described with the following equations of motion:

$$(m_c + m_p)\,\ddot{x} + m_p\, l \cos\phi\, \ddot{\phi} - m_c\, \dot{\phi}^2 \sin\phi = u, \tag{3.1}$$

$$m_c\, l \cos\phi\, \ddot{x} + m_p\, l^2 \ddot{\phi} + b\,\dot{\phi} - m_p\, l\, g\, \sin\phi = 0, \tag{3.2}$$

where m_c is the mass of the cart, b a damping constant representing friction in the joint of the pole and g represents the acceleration due to gravity. The mass of the pole is assumed to be concentrated in a point mass, m_p, at a distance l of the joint. For simplicity constants will be set at the value 1, except b and g. The value of b will be used as a tuning parameter and g is fixed at 9.81 $\left[\frac{\mathrm{m}}{\mathrm{s}^2}\right]$. The equations of motion (3.1) and (3.2) can be written as:

$$2\,\ddot{x} + \cos\phi\, \ddot{\phi} - \dot{\phi}^2 \sin\phi = u, \tag{3.3}$$

$$\cos\phi\, \ddot{x} + \ddot{\phi} + b\,\dot{\phi} - 9.81\, \sin\phi = 0. \tag{3.4}$$

3.3 Simulations with Partial Feedback Linearization

In order to enable simulations with PFL, the equations (3.3) and (3.4) have to be translated to the description used in Section 2.2. This results in the following relations:

$$\begin{array}{lll} M_{aa} = 2 & h_a = -\dot{\phi}^2 \sin\phi & f_a = 0 \\ M_{ap} = M_{pa} = \cos\phi & h_p = 0 & f_p = b\,\dot{\phi} - 9.81\, \sin\phi \\ M_{pp} = 1. & & \end{array}$$

Controlling the position; the collocated case

To show that it is possible to gain insight in the behavior of the uncontrolled DOF before explicit simulation of the controlled system behavior, we first investigate the zero dynamics of the closed loop system. Therefore, the system values are substituted in Eq. 2.11. This results in the following equation describing the zero dynamics of the closed loop system of the cart-pole .

$$\ddot{\phi} = -b\,\dot{\phi} + 9.81\, \sin\phi - cos(\phi)\ddot{x}_d. \tag{3.5}$$

The desired position x_d is chosen as $x_d = 0$, $\dot{x}_d = 0$ and $\ddot{x}_d = 0$. With this choice the zero dynamics of the closed loop system can be rewritten as:

$$\ddot{\phi} = -b\dot{\phi} + 9.81 \sin\phi, \tag{3.6}$$

where b is still variable. To show the use of phase portraits in a situation like this, Eq. (3.6) is examined at two values of b, namely $b = 0$ $\left[\frac{\text{Ns}}{\text{m}}\right]$ and $b = 0.1$ $\left[\frac{\text{Ns}}{\text{m}}\right]$. The phase portraits of the two situation are displayed in Figure 3.2.

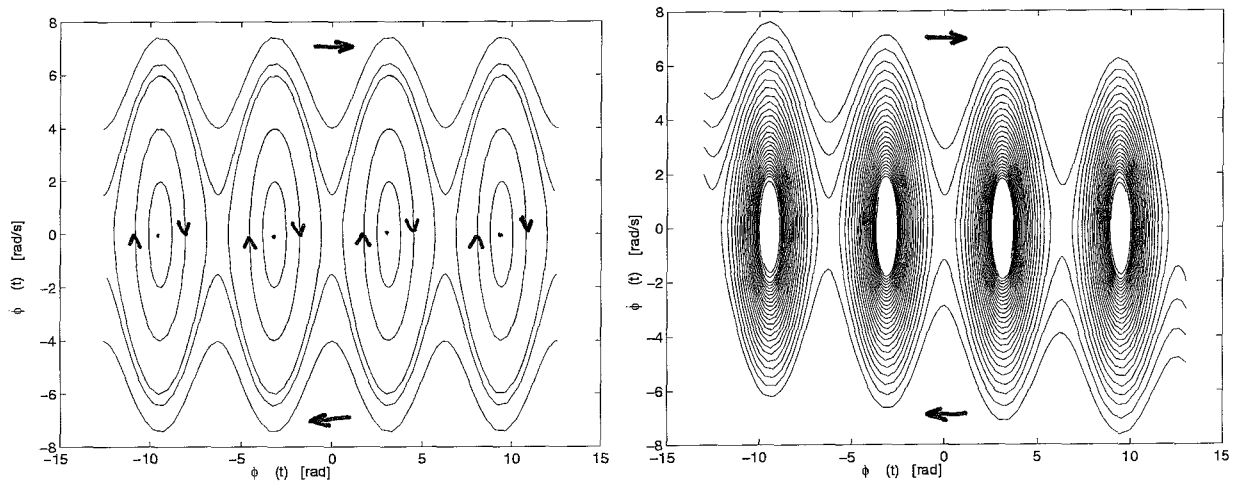

(a) $b = 0$.

(b) $b = 0.1$.

Figure 3.2: Phase portraits of the zero dynamics of the closed loop system when controlling the position.

For the situation that $b = 0$ $\left[\frac{\text{Ns}}{\text{m}}\right]$, it is possible to distinguish two different types of trajectories for the pole, when the cart has reached the desired position. The first type, is presented by centers in the phase plane. The pole swings between two angles of the same absolute magnitude. When the pole follows the second trajectory type it will turn around, giving a continuous increase or decrease of the angle ϕ. When following such a trajectory, the behavior of the pole is strictly speaking unstable. But, as we will see, it is still possible to control the position of the cart. So the in- or decrease of the angle does not lead to undesired system behavior and therefore the behavior of the pole can be called limited stable. Which path the pole follows in the phase plane will be determined by the starting point and the control gains. The desired angle is in this situation not stable when the cart is in rest. Therefore it will not be possible to satisfy the part of the control goal concerning the uncontrolled DOF, when $b = 0$ $\left[\frac{\text{Ns}}{\text{m}}\right]$, except for the case when the zero dynamics is entered exactly on $\dot{\phi} = 0$ and $\phi = \pi + n2\pi$ and $n \in \mathcal{Z}$.

For the situation that $b = 0.1$ $\left[\frac{\text{Ns}}{\text{m}}\right]$, an infinite number of stable foci occur. The pole will always end with the top aimed downwards, for the angle $\phi = \pi + n2\pi$ and $n \in \mathcal{Z}$, satisfying the part of the control goal that concerns the uncontrolled DOF. The pole will usually turn round a few times before it starts swinging and finally ends in a stable end position. The behavior of the pole depends on where the system enters the phase plane which is determined by the control gains and the initial condition. How smaller the angle speed for the same angle is, at the time that the controlled DOF has reached its objective, how faster the pole will damp out.

After examining the zero dynamics of the closed loop system, simulations are carried out to realize the control goal. The input for these simulations is determined with Eq. (2.5). Substituting the values of the cart-pole, the following equation is obtained:

$$u = (2 - \cos^2\phi)\ v - \dot{\phi}^2 \sin\phi - \cos\phi\,(b\,\dot{\phi} - g\,\sin\phi), \tag{3.7}$$

where v is a new input. This new input is chosen similar to Eq. (2.8), and results in:

$$v = -k_d\dot{x} - k_p x, \tag{3.8}$$

where k_d and k_p are the control gains for the error feedback. Furthermore, an initial condition for the cart-pole has to be chosen. We choose the following initial values for the state variables: $x_0 = 2$ [m], $\phi_0 = 0$ [rad], $\dot{x}_0 = 0\ [\frac{\text{m}}{\text{s}}]$ and $\dot{\phi}_0 = 0\ [\frac{\text{rad}}{\text{s}}]$.

The simulation results of two sets of control gains ($k_d = 20$, $k_p = 100$ and $k_d = 100$, $k_p = 100$) are presented in Figure 3.3. This choice seems rather arbitrary, but leads to insight in the influences of the parameter choice. The first interesting thing is the behavior of the controlled DOF which is the same regardless the value of damping. This is caused by the fact that the input compensates for the behavior of the pole.

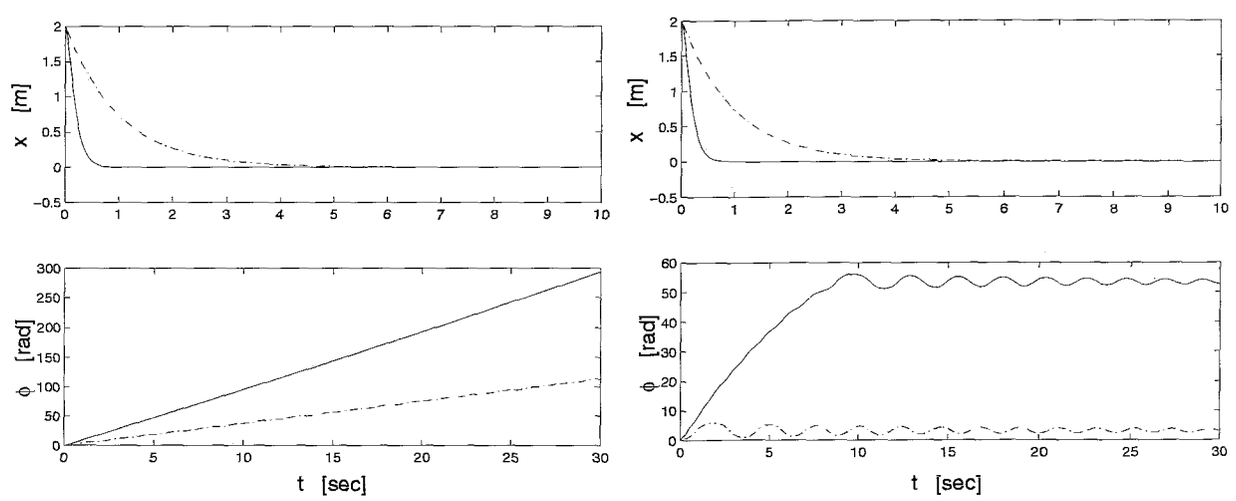

(a) $b = 0$.

(b) $b = 0.1$.

Figure 3.3: The behavior of x and ϕ for different damping values, where the solid line represents ($k_d = 20$, $k_p = 100$ and the dash-dotted line represents $k_d = 100$, $k_p = 100$).

For both values of b, we see the behavior of the pole as expected after the investigation of the zero dynamics of the closed loop system. When $x = x_d$ the input only compensated for the influence of ϕ on x, to keep $x = x_d$. The behavior of ϕ is determined by the system properties which are described by the zero dynamics of the closed loop system. The zero dynamics of the closed loop system can, therefore, be used to investigate the behavior of the uncontrolled DOF. It provides information whether the control goal for the uncontrolled DOF can be realized. For the situation that $b = 0\ [\frac{\text{Ns}}{\text{m}}]$ it is shown that it is not possible to satisfy the control goal for the uncontrolled DOF except for the case when the zero dynamics is entered exactly on $\dot{\phi} = 0$ and $\phi = \pi + n2\pi$ and $n \in \mathcal{Z}$, because otherwise the movement of the pole goes on 'for ever', as a result of the lack of damping in the joint of the pole. In the remaining of this chapter we will

only use the situation where $b = 0.1$ $[\frac{\text{Ns}}{\text{m}}]$. For that situation, the control goal for the uncontrolled DOF can be realized, as follows from the investigation of the zero dynamics of the closed loop system.

Now we return to the influence of the control gains on the behavior of the DOFs. Comparing the two sets of control gains we see that if the desired position is reached fast, it takes a long time for the pole to reach its rest position($k_d = 20$ and $k_p = 100$). This in contrast to a slow behavior of the cart ($k_d = 100$ and $k_p = 100$). Informally speaking, it can be said that good performance for one DOF results in bad performance for the other DOF. By looking at the poles of the error equation the choice for the control gain can be related to the behavior of the system. The error equation is given by:

$$\ddot{e}_x + k_d \dot{e}_x + k_p e_x = 0. \tag{3.9}$$

Poles of Eq. (3.9) placed far in the left-half plane represents a relatively fast convergence of e_x to zero, resulting in a fast moving cart. The cart passes this movement to the pole, resulting in a fast moving pole. This behavior corresponds with the control gains, $k_d = 20$ and $k_p = 100$ and the following poles -10 and -10. The control gains $k_d = 100$ and $k_p = 100$ with the poles -98.99 and -1.01 lead to a longer period for the cart to reach the desired position which results in a slower moving pole.

Controlling the angle; the non-collocated case

Before the zero dynamics of the closed loop system is examined, we check if the system is locally inertially coupled. Only if this condition is satisfied, it is possible to control the passive DOF (the angle of the pole) with PFL. The inertial coupling requires that M_{pa} has full rank. This leads to the following restriction for ϕ:

$$M_{pa} = \cos\phi \neq 0.$$

If ϕ is restricted to $-\frac{1}{2}\pi < \phi < \frac{1}{2}\pi$, M_{pa} has full rank which satisfies the inertial coupling condition. The restriction that the number of passive DOFs have to be equal or smaller to the numbers of inputs is also satisfied, because there is one passive DOF and one input. So the control of the angle is possible when the range of ϕ is restricted.

To investigate the behavior of the position, when the pole has reached the desired angle, the zero dynamics of the closed loop system is examined. To make this examination possible, Eq. (2.20) is used, resulting in:

$$\ddot{x} = \frac{-1}{\cos\phi_d}(\ddot{\phi}_d + b\dot{\phi}_d - g\sin\phi_d). \tag{3.10}$$

Choosing the desired angle as $\phi_d = 0$, $\dot{\phi}_d = 0$ and $\ddot{\phi}_d = 0$, while combined with Eq. (3.10), results in the following equation describing the zero dynamics of the closed loop system when the pole is controlled:

$$\ddot{x} = g\tan\phi_d = 0. \tag{3.11}$$

The phase portrait of Eq. (3.11) is shown in Figure 3.4.

Looking at the phase portrait, we see that when the pole reaches the desired angle, the position of the cart will keep increasing or decreasing with a constant speed. This behavior is strictly speaking not stable, but doesn't leads to unacceptable system behavior. Therefore, the behavior is called limited stable.

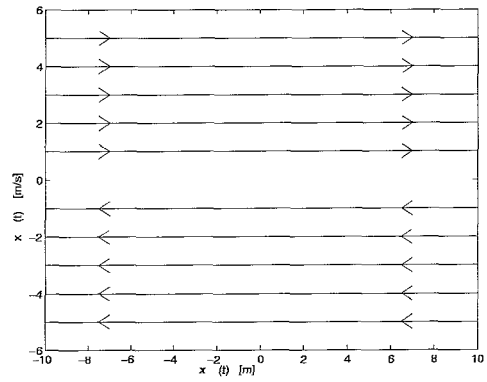

Figure 3.4: Phase portrait of the zero dynamics of the closed loop system when controlling the angle.

Eq. (2.14) is used to determine the input for simulation. The control input u becomes:

$$u = (\cos\phi - \frac{2}{\cos\phi})\, v - \dot{\phi}^2 \sin\phi - \frac{2}{\cos\phi}(\dot{\phi} - 9.81 \sin\phi), \tag{3.12}$$

where v is a new input. To guarantee asymptotically stable tracking, the input v is chosen similar to Eq. (2.17), resulting in:

$$v = -k_d\dot{\phi} - k_p\phi. \tag{3.13}$$

The control gains are chosen rather arbitrary as: $k_d = 20$ and $k_p = 100$. This is done, because the only interest in this situation is to see if it is possible to control the angle from the initial angle, $\phi_0 = \frac{\pi}{4}$ [rad], to the desired angle, $\phi_d = 0$ [rad]. The system behavior with these control gains is presented in Figure 3.5. The increasing position of the cart causes no problems, because x does not appear in the input and therefore does not lead to an increasing input.

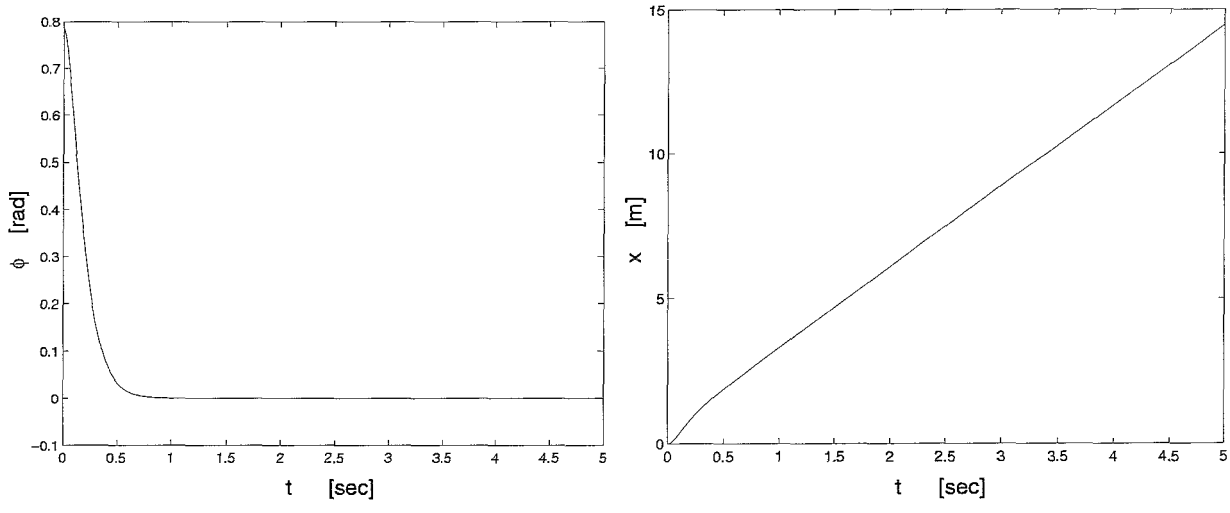

Figure 3.5: The system behavior when controlling the angle.

3.4 Simulations with Computed Desired Computed Torque Control

To be able to simulate with CDCTC, the cart-pole system as described by Eq. (3.3) and (3.4), has to be translated to the system description as used in Section 2.3. This results in the following matrices:

$$M = \begin{bmatrix} 2 & \cos\phi \\ \cos\phi & 1 \end{bmatrix}, \quad C = \begin{bmatrix} 0 & -\dot{\phi}\sin\phi \\ 0 & 0 \end{bmatrix}, \quad B = \begin{bmatrix} 0 & 0 \\ 0 & b \end{bmatrix},$$

$$f_n = \begin{bmatrix} 0 \\ -g\sin\phi \end{bmatrix}, \quad H = \begin{bmatrix} 1 \\ 0 \end{bmatrix}, \quad N = \begin{bmatrix} 0 \\ 1 \end{bmatrix}.$$

It is possible with CDCTC to determine the equations for computing the input and the desired trajectory for the uncontrolled DOF, before deciding which DOF is controlled. This is done by substituting the system values in Eq. (2.32) and (2.33). When the control gains K_d and K_p are chosen as diagonal matrices, this results in:

$$u = 2\ddot{x}_d + \cos\phi\,\ddot{\phi}_d - \dot{\phi}\,\dot{\phi}_d\sin\phi + k_{d_x}\dot{e}_x + k_{p_x}e_x, \tag{3.14}$$

$$0 = \cos\phi\,\ddot{x}_d + \ddot{\phi}_d + b\dot{\phi}_d - g\sin\phi + k_{d_\phi}\dot{e}_\phi + k_{p_\phi}e_\phi, \tag{3.15}$$

where k_{d_x}, k_{d_ϕ}, k_{p_x} and k_{d_ϕ} are the diagonal elements of K_d and K_p and the errors are defined as:

$$e_x = x_d - x, \qquad e_\phi = \phi_d - \phi. \tag{3.16}$$

Eq. (3.14) is used to compute the control input while Eq. (3.15) is used compute the desired trajectory for the uncontrolled DOF.

Controlling the position; the collocated case

Whether the position can be controlled with CDCTC depends on the ability to calculate a bounded desired trajectory for the angle using Eq. (3.15). Rewriting this equation results in:

$$\ddot{\phi}_d + (b + k_{d_\phi})\dot{\phi}_d + k_{p_\phi}\phi_d = \cos\phi\,\ddot{x}_d + g\sin\phi + k_{d_\phi}\dot{\phi} + k_{p_\phi}\phi. \tag{3.17}$$

The system values together with the control gains result in a stable differential equation for ϕ_d, which makes it is possible to compute the bounded desired trajectory on-line.

To compare CDCTC in a later stage with PFL, the initial condition and the desired trajectory for the position have to be the same as for PFL. The cart is again controlled from 2 [m] to 0 [m] and is initially at rest. Besides the initial condition also initial values for ϕ_{d_0} and $\dot{\phi}_{d_0}$ have to be chosen. These values are (as mentioned in Section 2.3) chosen the same as the corresponding values for the initial condition, namely $\phi_{d_0} = 0$ [rad] and $\dot{\phi}_{d_0} = 0\left[\frac{\text{rad}}{\text{s}}\right]$.

Before doing simulations with CDCTC, four control gains have to be chosen. Two, concerning the feedback of position errors (k_{d_x} and k_{p_x}), and two for the feedback of angle errors (k_{d_ϕ} and k_{p_ϕ}). To compare the simulation results in a later stage in a fair way with PFL, the choice for k_{d_x} and k_{p_x} is constrained. We want that the choice results in the same feedback for $\dot{e}_x$ and e_x as with PFL. In that way the difference between CDCTC and PFL, the extra contribution to the input caused by the feedback of e_ϕ, appears. To find values for k_{d_x} and k_{p_x} that accomplish the same feedback, the error equation (2.39) is used and rewritten as:

$$\ddot{e}_x + \frac{1}{2-\cos^2\phi}(k_{d_x}\dot{e}_x + k_{p_x}e_x - (\dot{\phi}\sin\phi + \cos\phi(k_{d_\phi} + b))\dot{e}_\phi - \cos\phi k_{p_\phi}e_\phi) = 0, \tag{3.18}$$

$$\ddot{e}_\phi + \frac{1}{2-\cos^2\phi}(-\cos\phi k_{d_x}\dot{e}_x - \cos\phi k_{p_x}e_x + (\dot{\phi}\sin\phi\cos\phi + 2(k_{d_\phi}+b))\dot{e}_\phi + 2k_{p_\phi}e_\phi) = 0. \quad (3.19)$$

By comparing Eq. (3.18) with Eq. (3.9), it follows that to realize the same feedback for $\dot{e}_x$ and e_x, the control gains for the position have to be chosen as:

$$k_{d_x} = (2-\cos^2\phi)k_d, \qquad k_{p_x} = (2-\cos^2\phi)k_p. \quad (3.20)$$

Eq. (3.20) can only be satisfied with time varying control gains. So, with constant values the same feedback of e_x and $\dot{e}_x$ cannot be realized. To compare CDCTC with PFL as good as possible, $2-\cos^2\phi$ in Eq. (3.20) ir replaced by its minimum value 1. This results in the following relations between the gains: $k_{d_x} = k_d$ and $k_{p_x} = k_p$ (for the values of k_d and k_p see previous section). Besides this, the gains for the angle feedback have to be chosen. We use the same two sets of values as used for the feedback of the position. With this choice we expect, as in Section 3.3, to gain insight. Combining the choices for k_{d_ϕ}, k_{p_ϕ} with those for k_{d_x}, k_{p_x}, leads to four sets of gains given below. Simulation results with these sets are presented in Figure 3.6.

set 1 :	$k_{d_x} = 20,$	$k_{p_x} = 100,$	$k_{d_\phi} = 20,$	$k_{p_\phi} = 100.$
set 2 :	$k_{d_x} = 20,$	$k_{p_x} = 100,$	$k_{d_\phi} = 100,$	$k_{p_\phi} = 100.$
set 3 :	$k_{d_x} = 100,$	$k_{p_x} = 100,$	$k_{d_\phi} = 20,$	$k_{p_\phi} = 100.$
set 4 :	$k_{d_x} = 100,$	$k_{p_x} = 100,$	$k_{d_\phi} = 100,$	$k_{p_\phi} = 100.$

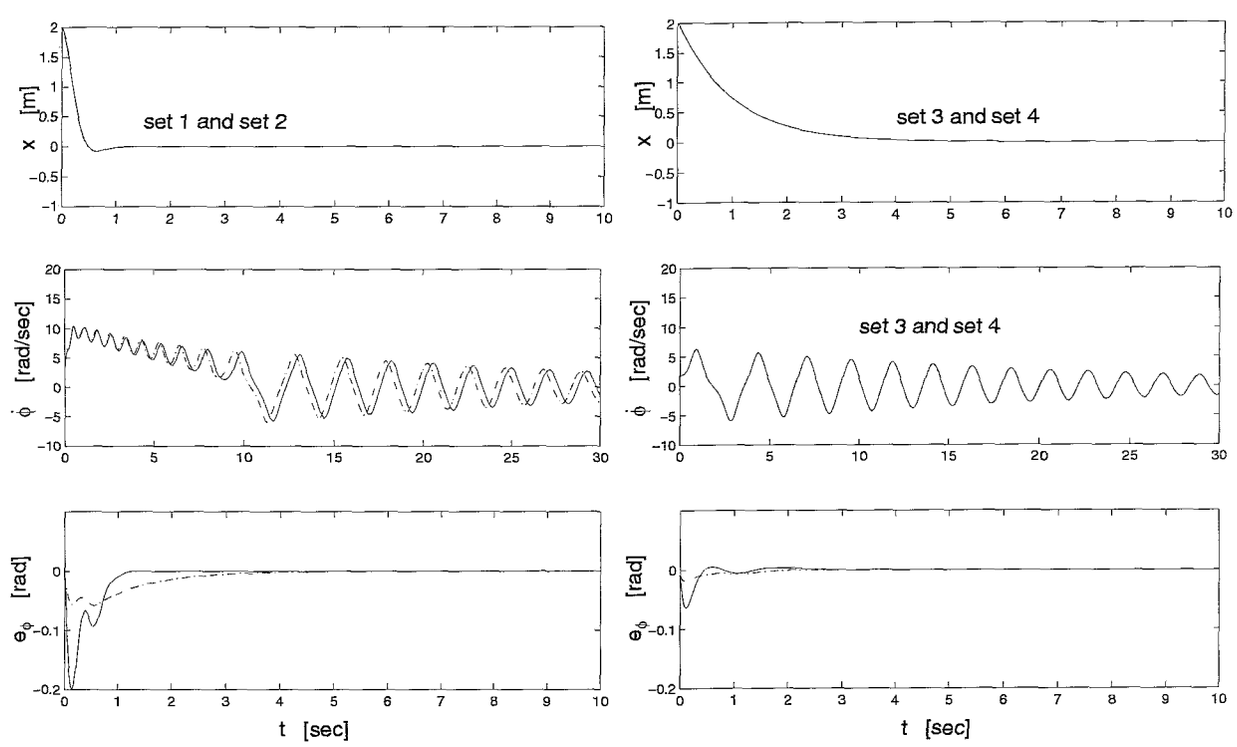

(a) Set 1 and set 2.

(b) Set 3 and set 4.

Figure 3.6: The behavior of x and $\dot{\phi}$ for different control gains; the solid line represents set 1 and set 3 and the dash-dotted line represents set 2 and set 4.

When $x = x_d$ the input compensates for the influence of ϕ to make sure that x remains equal to x_d. Looking at the influence of k_{d_x} and k_{p_x}, we see that again fast control of the position leads to the pole reaching

the rest position slowly (set 1 and set 2), in contrast to slow control for the position where the angle comes quicker to rest (set 3 and set 4). The influence of the gains on the feedback of the angle is not so clear. Looking at set 1 and set 2 we notice that the performance of the angle can be improved a little with set 2. This set results also in a slower convergence of e_ϕ to zero. It is expected that the extra input contribution, as a result of the feedback of the angle error, effects the system longer and has a positive effect on the behavior for a longer period of time. Looking at set 3 and set 4 we notice the same behavior regardless the choice for the angle feedback. A probable explanation is that the feedback of the angle errors is too small to influence the behavior.

To see if the improvement of the performance can be enlarged, the feedback of the angle errors is increased. This can be realized with the following choice for the gain matrices (in contrast with the earlier used diagonal matrices).

$$K_d = \begin{bmatrix} k_{d_x} & k_{d_e} \\ 0 & k_{d_\phi} \end{bmatrix}, \quad K_p = \begin{bmatrix} k_{p_x} & k_{p_e} \\ 0 & k_{p_\phi} \end{bmatrix}, \tag{3.21}$$

where one element is chosen zero. Through examining the influence of k_{d_e} and k_{p_e} for set 2 and set 4, the influence of the extra gains is examined for fast and slow control of the position and those gains for the angle feedback that can result in better performance. Simulations with several values of k_{d_e} and k_{p_e} resulted in the conclusion that these gains can be chosen negative, but the absolute magnitude of these gains cannot be chosen freely. When the absolute magnitude is too large the system behavior becomes unstable. The values that are used for the simulations presented in Figure 3.7 are roughly the largest that still lead to desired system behavior.

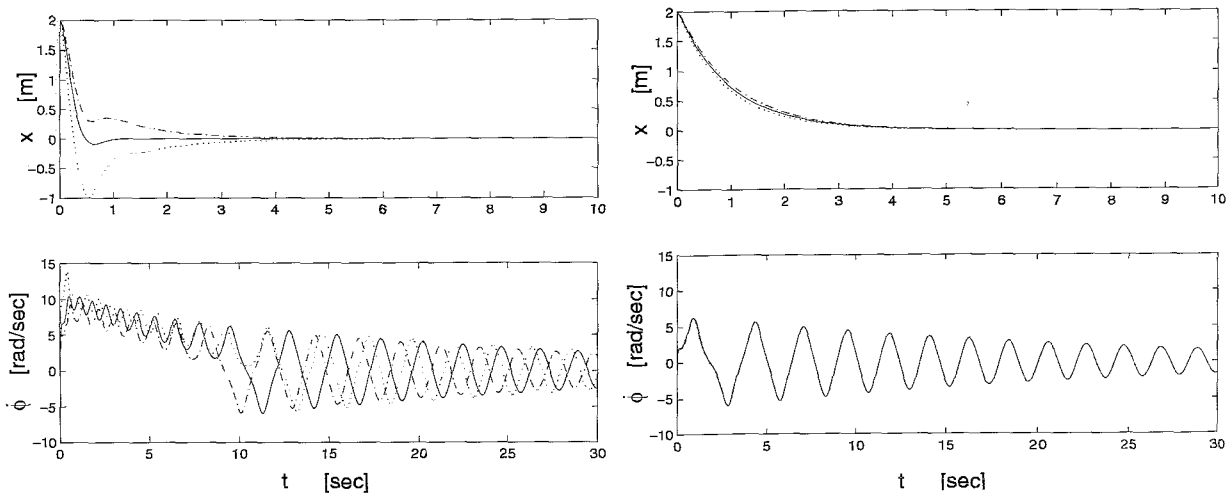

(a) $k_{d_x} = 20, k_{p_x} = 100, k_{d_\phi} = 100$ and $k_{p_\phi} = 100$ (set 2).

(b) $k_{d_x} = 100, k_{p_x} = 100, k_{d_\phi} = 100$ and $k_{p_\phi} = 100$ (set 4)

Figure 3.7: The behavior of x and $\dot{\phi}$ for different gains, where the solid line represents $k_{d_e} = 0$ and $k_{p_e} = 0$, the dotted line represents $k_{d_e} = 100$ and $k_{p_e} = 1000$ and the dash-dotted line represents $k_{d_e} = -100$ $k_{p_e} = -1000$.

In Figure 3.7a can be seen that a smart choice, $k_{d_e} = -100$ and $k_{p_e} = -1000$, can improve the behavior of the pole, where the other set of extra gains has a negative effect on the performance. Furthermore, it is notices that the improvement of the behavior of the pole implies a decreasing performance of the cart.

The extra input contribution caused by the feedback of the angle errors with $k_{d_e} = -100$ and $k_{p_e} = -1000$ leads to better performance for the pole. In Figure 3.7b can be seen that extra feedback of the angle errors does not result in a chance in the behavior.

Controlling the angle; the non-collocated case

Whether it is possible to use CDCTC to control ϕ, depends on the possibility to compute a bounded desired trajectory for x. To see if this is possible we rewrite Eq. (3.24) which results in:

$$\cos\phi\,\ddot{x}_d = -\ddot{\phi}_d - b\,\dot{\phi}_d + g\,\sin\phi - k_{d_\phi}\,\dot{e}_\phi - k_{p_\phi}\,e_\phi. \tag{3.22}$$

It is possible to compute $\ddot{x}_d$, and by numerical integration, $\dot{x}_d$ and x_d, as long as $\cos\phi \neq 0$. This condition is satisfied when the angle is restricted to $-\frac{1}{2}\pi < \phi < \frac{1}{2}\pi$. So with this restriction for the angle it is possible to use CDCTC to control the pole. Simulation also show that control of the pole leads to the desired behavior for the pole as the angle is restricted (see Figure 3.8).

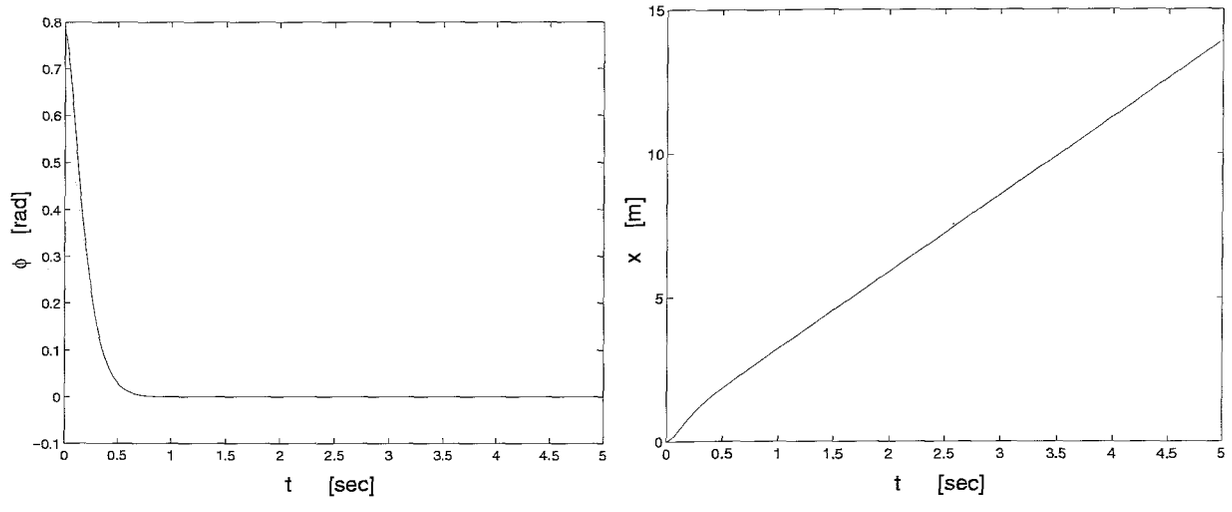

Figure 3.8: The system behavior when controlling the angle using CDCTC, where $k_{d_x} = 100$, $k_{d_\phi} = 20$, $k_{d_x} = 100$, and $k_{d_\phi} = 100$.

3.5 Simulations with Computed Reference Computed Torque Control

As we have seen in the previous chapter, CRCTC is strongly related to CDCTC. The only difference is the usage of a reference trajectory instead of a desired trajectory.

As with CDCTC it is possible to determine the equations for computing the input, and a reference trajectory, before we choose which of the two DOFs is controlled. Therefore, the system values are substituted in Eq. (2.40) and (2.41). With K_r chosen diagonal for simplicity, this results in:

$$u = 2\,\ddot{x}_r + \cos\phi\,\ddot{\phi}_r - \dot{\phi}\,\dot{\phi}_r\,\sin\phi_o + k_{r_x}\,\dot{e}_{x_r}, \tag{3.23}$$

$$0 = \cos\phi\,\ddot{x}_r + \ddot{\phi}_r + b\,\dot{\phi}_r - g\,\sin\phi + k_{r_\phi}\,\dot{e}_{\phi_r}, \tag{3.24}$$

where k_{r_x} and k_{r_ϕ} are the diagonal elements of K_r, and the reference trajectories are defined as:

$$\begin{array}{lll} \dot{x}_r = \dot{x}_d + \Lambda_x e_x, & e_x = x_d - x, & e_{x_r} = x_r - x, \\ \dot{\phi}_r = \dot{\phi}_d + \Lambda_\phi e_\phi, & e_\phi = \phi_d - \phi, & e_{\phi_r} = \phi_r - \phi. \end{array} \tag{3.25}$$

Whether Eq. (3.24) is used to compute x_r or ϕ_r depends on which DOF is controlled.

Controlling the position; the collocated case

As with CDCTC the first step is to see if it is possible to control the position with CRCTC. Or, is it possible to compute a bounded reference trajectory for the angle? To answer this question, Eq. (3.24) is rewritten as:

$$\ddot{\phi}_r + (b + k_{r_\phi})\dot{\phi}_r = \cos\phi \ddot{x}_r + g \sin\phi + k_{r_\phi}\dot{\phi}. \tag{3.26}$$

Whether a bounded reference trajectory can be computed with Eq. (3.26) depends on the system values together with the control gains. The system values and control gains used in this study result in a stable differential equation for ϕ_d, which makes it is possible to compute the trajectory on-line and, thus, to use CRCTC to control the position of the cart-pole system.

For a good comparison between PFL and CRCTC, the initial conditions and the desired position are chosen the same as in earlier simulations. The cart is at rest at t=0 [sec] and the goal is to control it from 2 [m] to 0 [m]. Furthermore, the initial conditions for the reference trajectories have to be chosen. These conditions are, as mentioned in Section 2.4, chosen the same as the corresponding values for the initial conditions for the cart and the pole, namely: $x_{r_0} = 2$ [m], $\phi_{r_0} = 0$ [rad] and $\dot{\phi}_{r_0} = 0 \left[\frac{\text{rad}}{\text{s}}\right]$.

The behavior of the cart-pole with CRCTC can be influenced, at first sight, by four control gains. Two for the feedback of the position k_{r_x} and Λ_x, and two for the feedback of the angle k_{r_ϕ} and Λ_ϕ. However, the reference trajectory for the angle is computed with Eq. (3.26) instead of Eq. (3.25) and so Λ_ϕ is not used to compute the reference trajectory for the angle. This results in the fact that the choice for Λ_ϕ does not influence the reference trajectory for the angle and so the system behavior cannot be influenced with Λ_ϕ. This leaves three control gains that can influence the behavior. As with CDCTC, k_{r_x} and Λ_x cannot be chosen freely. To compare CRCTC with PFL in a later stage, the feedback of $\dot{e}_x$ and e_x is chosen the same as with PFL. To find a relation for the control gains, the reference error equation is given by:

$$\ddot{e}_{x_r} + \frac{1}{2 - \cos^2\phi}(k_{r_x}\dot{e}_{x_r} - (\dot{\phi}\sin\phi + \cos\phi(k_{r_\phi} + b))\dot{e}_{\phi_r}) = 0, \tag{3.27}$$

$$\ddot{e}_{\phi_r} + \frac{1}{2 - \cos^2\phi}(-\cos\phi k_{r_x}\dot{e}_{x_r} + (\dot{\phi}\sin\phi\cos\phi + 2(k_{r_\phi} + b))\dot{e}_{\phi_r}) = 0. \tag{3.28}$$

Substituting the definitions for $\ddot{e}_{x_r}$ and $\dot{e}_{x_r}$ in Eq. (3.27) and comparing it with Eq. (3.9), results in the following equations for k_{r_x} and Λ_x.

$$k_{r_x} + (2 - \cos^2\phi)\Lambda_x = (2 - \cos^2\phi)k_d, \qquad k_{r_x}\Lambda_x = (2 - \cos^2\phi)k_p. \tag{3.29}$$

It is not possible to realize the same feedback for $\dot{e}_x$ and e_x , with constant values for the control gains. To make a comparison possible, $2 - \cos^2\phi$ is replaced in Eq. (3.29), as was the case for CDCTC, by 1. Solving the new equations for the two sets of gains used in Section 3.3 leads to the following two sets: $k_{r_x} = 10$, $\Lambda_x = 10$, and $k_{r_x} = 99$, $\Lambda_x = 1$. The last control gain, yet to be chosen is k_{r_ϕ}. To get insight in the influence of this control gain, a small value $k_{r_\phi} = 0.1$, and a larger one $k_{r_\phi} = 20$ is used, for both sets of k_{r_x} and Λ_x. The simulations are displayed in Figure 3.9. Besides the already given initial condition, also

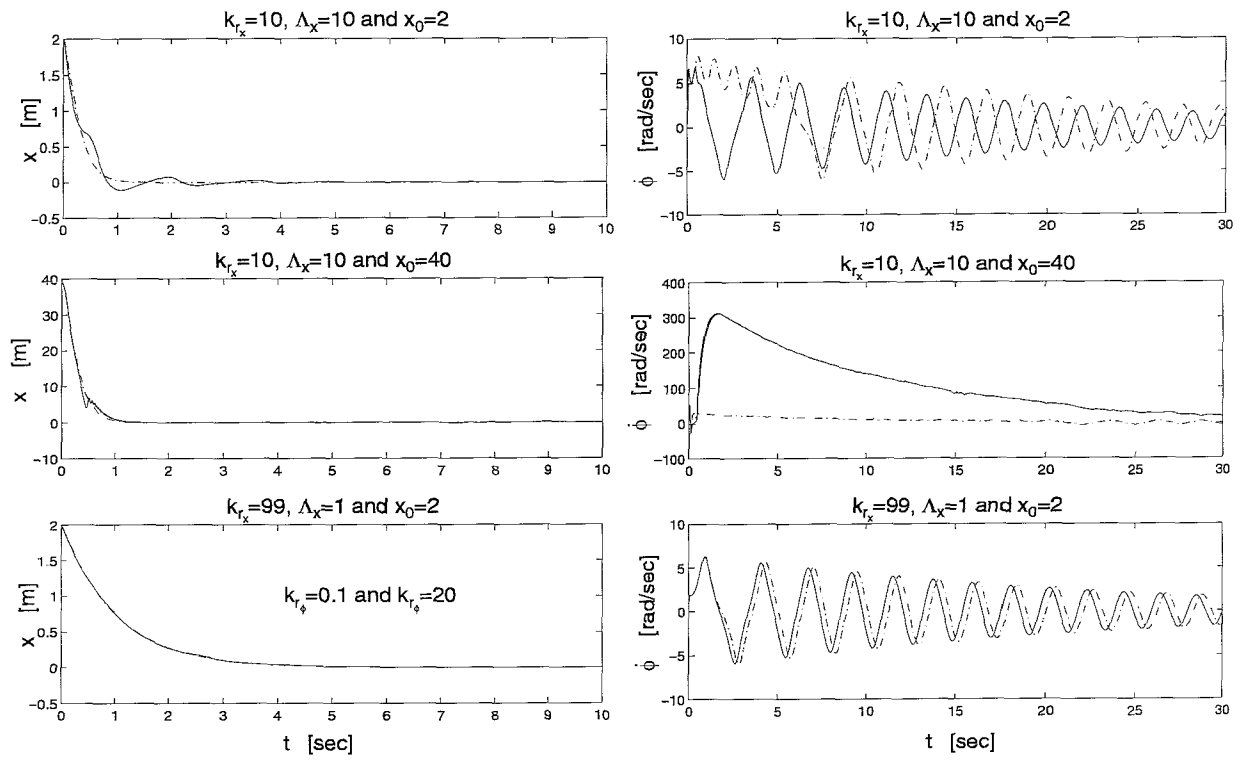

Figure 3.9: The behavior of x and $\dot{\phi}$ for different control gains and initial conditions, where the solid line represents the situation where $k_{r_\phi} = 0.1$ and the dash-dotted line represents the situation where $k_{r_\phi} = 20$.

a simulation is presented with the initial position 40 [m] instead of 2 [m], to show the complete influence of the control gains.

Looking at the simulations, fast control of the cart implies slow control of the pole whereas slow control of the cart implies fast control of the pole. Again we notice that when $x = x_d$ the system can no longer be influenced by the input as is has to compensate exactly for the uncontrolled DOF in order to keep x equal to x_d. Our main interest is the influence of k_{r_ϕ} on the performance. For the simulations where the initial condition $x_0 = 2$ [m] (see Figure 3.9) we see that a small value for k_{r_ϕ}, causes $\dot{e}_{\phi_r}$ to converge slowly to zero, resulting in a better performance for the pole. This improvement for the behavior of the pole results in a decreasing performance of the cart. Again, as with CDCTC, the extra input contribution, caused by the feedback of the angle errors, influences the behavior in a positive way. However, the influence of this extra input contribution can change when the initial conditions change (for example $x_0 = 40$ [m] instead of $x_0 = 2$ [m]). A possible explanation for this is that the extra input contribution, caused by the feedback of the angle errors, cannot really be influenced.

To see if the improvement of the behavior can be enlarged using extra feedback on the angle errors (when $x_0 = 2$ [m]), K_r is chosen as:

$$K_r = \begin{bmatrix} k_{r_x} & k_{r_e} \\ 0 & k_{r_\phi} \end{bmatrix}. \tag{3.30}$$

Through simulations for several values for k_{r_e}, the same behavior as with CDCTC is noticed. Negative values improve the behavior of the pole and positive values decreasing the performance of the pole. Furthermore, the system behavior becomes unstable when the absolute magnitude of k_{r_e} is too large. The

simulations presented in Figure 3.10, are carried out with the initial condition $x_0 = 2$ [m] while for the control gains (except k_{r_e}), the set is used that performs the best for fast control of x (Figure 3.9), and the set that performs the best for slow control of x (Figure 3.9). This results in the following two sets of values for the gains: $k_{r_x} = 10$, $k_{r_\phi} = 0.1$, $\Lambda_x = 10$, and $k_{r_x} = 99$, $k_{r_\phi} = 0.1$, $\Lambda_x = 1$. For k_{r_e} a value is chosen that gives best performance.

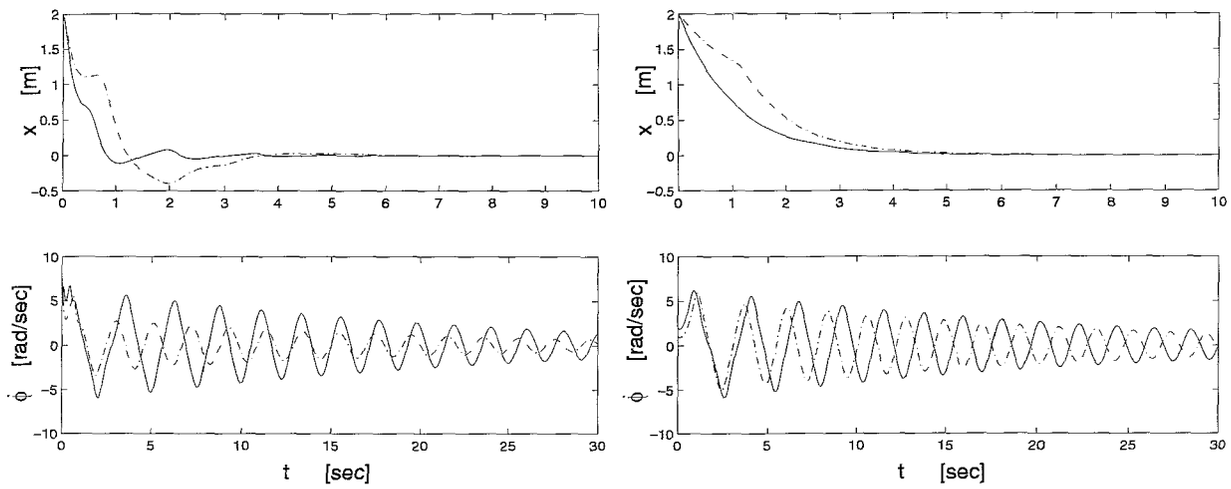

(a) $k_{r_x} = 10$, $k_{r_\phi} = 0.1$ and $\Lambda_x = 10$.

(b) $k_{r_x} = 99$, $k_{r_\phi} = 0.1$ and $\Lambda_x = 1$.

Figure 3.10: The behavior of x and $\dot{\phi}$ for different extra gains, where for the solid line $k_{r_e} = 0$ and for the dash-dotted line on the lefthand side $k_{r_e} = -10$ and on the righthand side $k_{r_e} = -100$.

The pole reaches in both situations the desired position father using the extra feedback of k_{r_e}. Looking at Figure 3.10a we notice that the gains $k_{r_x} = 10$, $\Lambda_x = 10$ $k_{r_\phi} = 0.1$ and $K_{r_e=10}$ result in a cart that is no longer controlled fast. But this goes together with a very good performance for the pole (even better than $k_{r_x} = 99$, $\Lambda_x = 1$ $k_{r_\phi} = 0.1$ and $k_{r_e} = -100$).

Controlling the angle; the non-collocated case

Whether it is possible to use CRCTC to control ϕ depends on the possibility to compute a bounded ϕ_r. To see if this is possible we rewrite Eq. (3.24), resulting in:

$$\cos\phi\,\ddot{x}_r = -\ddot{\phi}_r - b\,\dot{\phi}_r + g\,\sin\phi - k_{r_\phi}\,\dot{e}_{\phi_r}. \tag{3.31}$$

This equation shows similarities with Eq. (3.22) when using CDCTC. To be able to compute a bounded ϕ_r, the angle has to be restricted to $-\frac{1}{2}\pi < \phi < \frac{1}{2}\pi$. With these restrictions it is possible to use CRCTC to control the pole. Simulations show that control of the pole with CRCTC leads to the desired behavior for the pole (see Figure 3.11).

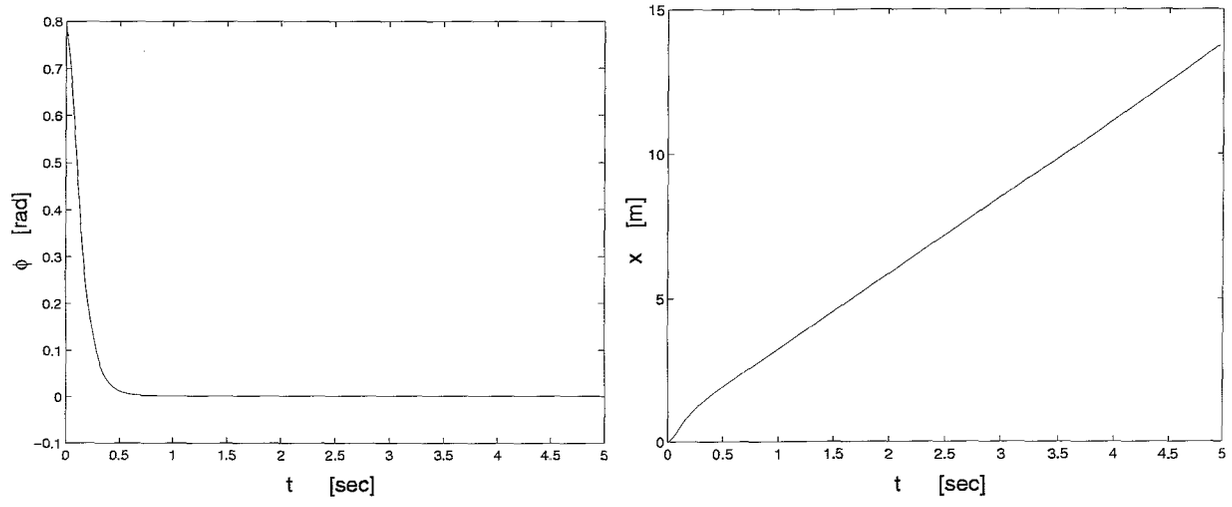

Figure 3.11: The system behavior when controlling the angle using CRCTC, where $k_{r_x} = 0.1$, $k_{r_\phi} = 10$ and $\Lambda_\phi = 10$.

3.6 Discussion

In this chapter three control methods have been used to control the cart-pole system. Only in the collocated case, when the position is controlled, the difference between PFL and CDCTC/ CRCTC appears. Therefore, the discussion is restricted to the collocated case, where the control goal is to get the cart from an initial position to the desired position, and to get the pole in the rest position as fast as possible. To make a comparison between the three methods possible, the two sets of PFL are printed together with the corresponding best sets of CDCTC, and CRCTC, in other words the sets that lead to almost the same feedback for the position errors.

The first control method that is used is PFL. To get insight in the behavior of the uncontrolled DOF the zero dynamics of the closed loop system is examined. When the behavior of the uncontrolled DOF is known, the conditions for good performance for the uncontrolled DOF can be derived. Simulations with PFL turned out that the requirements for the position and the pole were contradicting. Quick control of the cart resulted in slow control of the pole and the other way round.

The Second control method that is used is CDCTC. CDCTC not only uses e_x for feedback, as with PFL but also e_ϕ, which results in an extra input contribution to influence the system behavior. To investigate the influence of this extra input contribution, CDCTC has to be compared with PFL when the feedback for e_x is chosen equivalent. This is not possible for the cart-pole system. However, the gains for the feedback of e_x are chosen in such a way that the feedback is close to that with PFL. In Figure 3.12a we see that the performance of the pole with CDCTC is slightly better than with PFL. In Section 3.3 is shown that extra feedback on e_ϕ (when K_d and K_p are not diagonal), results in a larger extra input contribution, and can improve the behavior of CDCTC. So, it is reasonable to assume that the improvement of CDCTC in comparison to PFL is caused by this extra input contribution. Whereas, the performance of CDCTC in Figure 3.12b is the same as that of PFL, there is no set of gains found that realized an extra input contribution that could change the behavior of the cart-pole. This is caused by the fact that the influence of the gains on the desired trajectory for the angle, and so the influence on the extra input contribution, remain unclear. It is only possible to influence the speed in which e_ϕ converges to zero, and to some extent to enlarge the extra input contribution by extra feedback. However, we are not able to manipulate the form, and so the

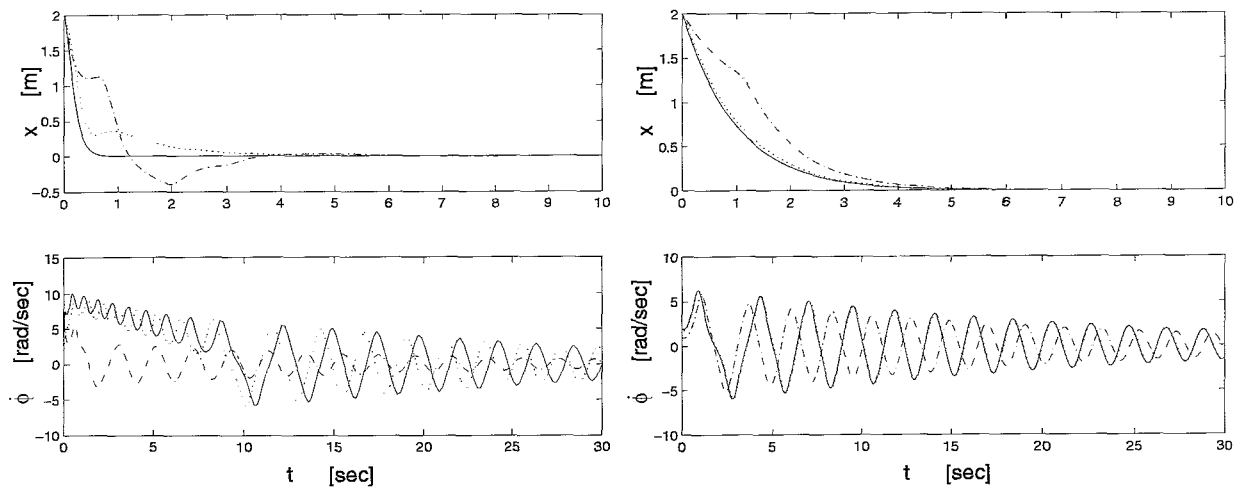

(a) PFL $\rightarrow$ $k_d = 20\,,\, k_p = 100.$
CDCTC $\rightarrow$ $k_{d_x} = 20, k_{p_x} = 100\,,\, k_{d_e} = -100,$
$k_{p_e} = -1000, k_{d_\phi} = 100, k_{p_\phi} = 100.$
CRCTC $\rightarrow$ $k_{r_x} = 10\,,\, k_{r_e} = -10\,,\, k_{r_\phi} = 0.1\ \Lambda_x = 10.$

(b) PFL $\rightarrow$ $k_d = 100, k_p = 100.$
CDCTC $\rightarrow$ $k_{d_x} = 100, k_{p_x} = 100, k_{d_e} = 0,$
$k_{p_e} = 0, k_{d_\phi} = 100, k_{p_\phi} = 100.$
CRCTC $\rightarrow$ $k_{r_x} = 99, k_{r_e} = -100, k_{r_\phi} = 0.1, \Lambda_x = 1.$

Figure 3.12: The behavior of x and $\dot{\phi}$ for the different control methods, where the solid line represents PFL, the dotted line represents CDCTC, and the dash-dotted line represents CRCTC.

influence, of the extra input contribution.

The last control method that is used is CRCTC. CRCTC uses, as with CDCTC, both the feedback of position errors and the feedback of the angle errors. In comparison to CDCTC, however, it uses $\dot{e}_{\phi_r}$ instead of e_ϕ. It is not possible to compare CRCTC in a fair way with PFL because it is not possible to realize the same error feedback for e_x with both control methods. The same approach, as with CDCTC in finding a smart relation between the gains of CRCTC concerning the feedback of the position and the gains of PFL, is used, making a sort of comparison possible. Looking at Figure 3.12a CRCTC performs much better than PFL, and CDCTC. As with CDCTC, the extra feedback on $\dot{e}_{\phi_r}$ (when K_r is not diagonal) can improve the behavior, and it is reasonable to assume that this improvement is caused by the extra input contribution. In Figure 3.12b is found that again the behavior is improved with CRCTC in comparison to PFL. But, this improvement is less then in Figure 3.12a. However, it is not possible to guarantee that there are no other sets of gains that perform better. This is caused by the fact that the influence of the extra input contribution is not understood. In Section 3.5 is found that for the same gains, a change of the initial condition resulted in a different extra input contribution. The reason for this is the fact that the extra input contribution cannot be influenced with the control gains in a structural way, so it is not possible to influence the system behavior in a user desired way.

Summarizing can be said that the best performance for the cart-pole is realized with CRCTC. There is no guarantee, however, that there are no sets for CDCTC and CRCTC that result in better performance. The lack of predictability of the influence of the extra input contribution makes it hard to find the best performance for the cart-pole. The unpredictability of the extra input contribution is a result of the dependency of the control gains and the initial conditions that influence in an unclear manner the extra input contribution. Furthermore, the extra input contribution cannot be understood physically because the desired/ reference trajectory is not physically interpretable.

Chapter 4

Control of the Beam with One-Sided Spring

4.1 Introduction

In the previous chapter we have seen how to control the cart-pole system with PFL, CDCTC and CRCTC, considering the influence of the control gains on the system behavior. Applying that knowledge the three control methods are used to realize vibration reduction for a nonlinear beam system. A description of the nonlinear beam system will be given in the next section. Here it is mentioned that the beam system has a one-sided spring attached to the middle where it is harmonically excited. From earlier studies it is known that the steady-state response has at least two natural solutions; a stable $\frac{1}{2}$ subharmonic solution of high vibration amplitude and an unstable harmonic solution of low vibration amplitude. Furthermore, the beam system has in principle an infinite amount of DOFs. From a computational point of view, this amount has to be reduced. Nevertheless, there still will be more DOFs than inputs, so we still have to deal with an underactuated system.

Trying to realize vibration reduction for the nonlinear beam system, the control goal is defined as: forcing the nonlinear beam system from a stable $\frac{1}{2}$ subharmonic solution into an unstable harmonic solution in a pre-defined time interval. We want to realize this vibration reduction for the entire beam, thus, for all DOFs. In the case that there are requirements for all DOFs, it is expected that CDCTC and CRCTC can perform better than PFL due to the possibility of error feedback for all the uncontrolled DOFs. Besides this we want to see if it is possible, with the control methods under study, to guarantee that all DOFs will follow the unstable harmonic solution of the beam. Up till now this was only possible for the controlled DOF, using (S)CTC, while it was assumed for the uncontrolled DOFs.

In this chapter we will derive a model of the nonlinear beam system, which will be followed by simulations with PFL to search for that set of gains that results in the best performance for the nonlinear beam system. After that, simulations with CDCTC will be given in order to improve the performance of PFL. The same will be done for CRCTC. These simulations will be followed by a discussion where the results of this chapter will be summarized. Furthermore, these results will be related to the cart-pole example of Chapter 3.

4.2 Model of the Beam with One-Sided Spring

In this section a short derivation of the model of the beam with one-sided spring is given. For more information concerning the beam and the derivation of the model the reader is referred to Fey [2]. The beam

with one-sided spring is schematically presented in Figure 4.1. The system consists of a beam (L=1.3 [m], W=0.01 [m] , H= 0.09 [m]) with a one-sided spring attached to the middle of the beam. When the displacement of the beam in the middle is positive, the one-sided spring results in an extra force acting on the system. The beam is harmonically excited in the middle. This excitation force is caused by a rotating mass unbalance. The control force can be applied with an actuator placed at a quarter of the beam.

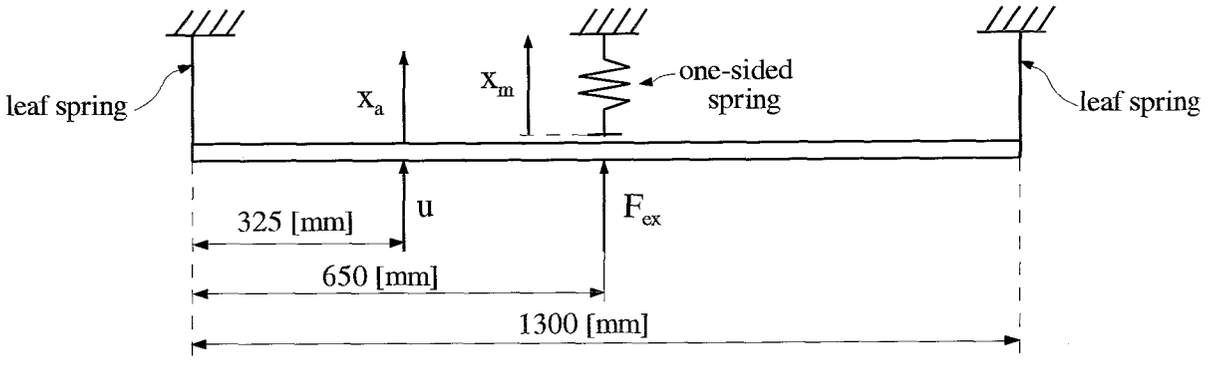

Figure 4.1: A schematical view of the nonlinear beam system.

As mentioned earlier, the beam has an infinitive amount of DOFs. To derive a model that can be used for simulations the number of DOFs has to be reduced. With the use of DIANA [1], a finite element package, a model of the beam is obtained. The linear beam is modeled with 86 finite elements resulting in 87 nodes, or DOFs. This amount of DOFs is still too large with respect to the calculation effort needed for the nonlinear analysis. The amount of DOFs is reduced with a component mode synthesis method (Vorst [9]). Damping is added to the reduced model by means of modal damping ζ, which is chosen equal for every mode ($\zeta = 0.02$). For practical reasons a 3-DOF model is obtained. The column $q = q(t)$, of the 3-DOF model, is defined as $q^T = [q_a(t)\ q_m(t)\ \xi(t)]$, where $q_a(t)$ is corresponding with the interface node for the control force, $q_m(t)$ is corresponding with the interface node for the one-sided spring and the excitation force, and $\xi(t)$ is a virtual DOF, corresponding with the first interface eigenmode of the reduced linear system. q_a is the active DOF while both q_m and ξ are passive DOFs. The 3-DOF model of the beam with one-sided spring, can be written as:

$$M\ddot{q} + B\dot{q} + Kq + H_1\, F_{nl}(q) = H_2\, F_e + H_3\, u, \tag{4.1}$$

where M is the mass matrix, B the damping matrix, K the stiffness matrix and H_1, H_2, H_3 the so-called 1×3 transition matrices. M, B, and K are symmetric positive definite matrices. For the values of the matrices see Appendix A. $F_{nl}(q)$ represents the one-sided spring and is defined as:

$$F_{nl}(q) = \varepsilon(q_m)\, k_{nl}\, q_m, \qquad \text{where} \qquad \varepsilon(q_m) = \begin{cases} 1, & \text{if } q_m \geq 0, \\ 0, & \text{if } q_m < 0, \end{cases} \tag{4.2}$$

with k_{nl} the stiffness of the one-sided spring, $k_{nl} = 1.65\ 10^5\ [\frac{\mathrm{N}}{\mathrm{m}}]$. The harmonic excitation force is given by:

$$F_e = m_e\, r_e\, \omega^2 \cos(\omega t), \qquad \omega = 2\pi\, f_e. \tag{4.3}$$

f_e is the excitation frequency and m_e is a rotating point mass at radius r_e, $m_e r_e$ is chosen as $0.984\ 10^{-3}$ [kg m].

From earlier studies it follows that this 3-DOF model describes the frequency behavior of the beam accurate up to an excitation frequency of 100 [Hz]. At the excitation frequency of 37 [Hz] two coexisting solutions exist. A stable $\frac{1}{2}$ subharmonic solution with a high amplitude and an unstable harmonic solution with a low amplitude. As mention in the introduction of this chapter the control goal is to control the system from the stable $\frac{1}{2}$ subharmonic solution to the unstable harmonic solution to obtain vibration reduction. An advantage of stabilizing the unstable harmonic response lies in the fact that it is a natural solution, which means that no control effort is needed once stabilized. With DIANA it is possible to calculate this unstable solution which represents the desired trajectory needed for control. The desired trajectory q_d is approximated using a truncated Fourier series. This enables easy derivation of the desired displacement, velocity, and acceleration during simulations. The Fourier coefficients needed for the approximation are given in Appendix A.

4.3 Simulation with Partial Feedback Linearization

The first control method that is used to realize vibration reduction for the beam system is PFL. The model of the beam system (Eq. (4.1)) has to be related to the system description used with PFL (Eq. (2.1) and (2.2)). This gives the following relations:

$$\begin{array}{lll} M_{aa} = M_{1,1}, & h_a = 0, & f_a = B_{1,1:3}\,\dot{q} + K_{1,1:3}\,q, \\ M_{ap} = M_{pa}^T = M_{1,2:3}, & h_p = 0, & f_{p_1} = B_{2,1:3}\,\dot{q} + K_{2,1:3}\,q + F_{nl} - F_e, \\ M_{pp} = M_{2:3,2:3}, & & f_{p_2} = B_{3,1:3}\,\dot{q} + K_{3,1:3}\,q, \end{array}$$

where the values for the system matrices are given in Appendix A. The DOFs have to be divided in controlled and uncontrolled DOFs. With PFL two cases can be distinguished. The first case, where the active DOF is the controlled DOF and the passive DOFs are the uncontrolled DOFs, is called the collocated case. In the second case the passive DOFs are chosen as the controlled DOFs. This case is called the non-collocated case.

Control of the actuator DOF; the collocated case

Before PFL is used to realize vibration reduction in simulations, the zero dynamics of the closed loop system is examined. This is done to gain insight in the behavior of the uncontrolled DOFs, and to see if the uncontrolled DOFs will reach there desired trajectories (the unstable harmonic response of the beam system). To investigate the zero dynamics of the closed loop system, the values of the beam system have to be substituted in Eq. 2.11. This results in the following equation:

$$M_{2:3,2:3}\ddot{q}_p + B_{2:3,2:3}\dot{q}_p + K_{2:3,2:3}\,q_p + H_{1_{2:3,1}}\,F_{nl} = H_{2_{2:3,1}}\,F_e - M_{2:3,1}\ddot{q}_{a_d} - B_{2:3,1}\,\dot{q}_{a_d} - K_{2:3,1}\,q_{a_d}. \quad (4.4)$$

Simulation of the zero dynamics of the closed loop system for several initial condition of q_p always resulted in the fact that q_p converged to the desired trajectory q_{p_d}, which made it reasonable to assume globally asymptotically stable behavior for q_p. Moreover, Sanders [6] showed, that this assumption can be justified from a theoretical point of view, by applying Popov's criterion (Slotine and li [7]).

To control q_a with PFL, the input u has to be determined. This results, using Eq. (2.5), in:

$$u = (M_{aa} - M_{ap}\,M_{pp}^{-1}\,M_{pa})\,v + h_a - M_{ap}\,M_{pp}^{-1}\,h_p + f_a - M_{ap}\,M_{pp}^{-1}\,f_p. \quad (4.5)$$

This input introduces a new input v that is chosen similar to Eq. (2.8), resulting in:

$$v = \ddot{q}_{a_d} + k_d\,(\dot{q}_{a_d} - \dot{q}_a) + k_p\,(q_{a_d} - q_a), \tag{4.6}$$

with two control gains $k_d \geq 0$ and $k_p \geq 0$ to influence the system behavior. To simulate the system behavior the initial conditions have to be chosen. For the initial condition the beam is set at rest at $t = 0$ [sec]. The first second no control is applied ($u = 0$ for $t < 1$ [sec]). This enables the beam to reach the stable $\frac{1}{2}$ subharmonic response with large vibration amplitude. At $t = 1$ [sec] the control is started so the beam is forced towards the unstable harmonic response, reducing vibration amplitude.

To find the gains that result in the best performance under the conditions as given above, a usable definition for the performance has to be derived. To quantify the performance, the time is used, needed for all DOFs to reach the desired unstable harmonic response. In practice it is not possible to find that time exactly due to numerical errors in the approximation of q_d. Therefore, the following definition is used: *the largest period t_i needed for the error, $abs(e_i) = (q_{i_d} - q_i)$, to become smaller than $e_{i_{max}}$ and remain smaller.* i represents one of the three DOFs. The value for $e_{i_{max}}$ is chosen at a 5% level of $\max(q_{i_d}) - \min(q_{i_d})$.

In order to stress out the influence of the gains, the error equation of the beam system, using PFL, is written as:

$$\ddot{e}_a + k_d\,\dot{e}_a + k_p\,e_a = 0, \tag{4.7}$$

where k_d and k_p are chosen as :

$$k_d = \lambda + \eta, \qquad k_p = \lambda\,\eta. \tag{4.8}$$

$-\lambda$ and $-\eta$ represent the poles of the error equation (4.7). The choice of the values for the gains is restricted to positive reals. When the poles are placed far in the left-half plane, q_{a_d} is reached fast. The influence of the gains on the behavior of the uncontrolled DOFs is not that obvious. It is obvious that q_p reaches its desired trajectory q_{p_d} always at a later time than q_a, due to the flexibility that connects q_p with q_a; in case of a rigid body q_{p_d} is reached at the same time as q_{a_d}. Furthermore, when q_a reaches q_{a_d} the input only compensates for the behavior of q_p to keep q_a at q_{a_d}. The behavior of q_p is completely determined by the system properties and will converge to q_{p_d}. How long it takes to reach q_{p_d} is determined by the values of q_p at the time that q_a reaches q_{a_d}, in other words the state in which the zero dynamics of the closed loop system is entered. Applying numerical studies, it was noticed that when q_a was controlled fast, this resulted in a bad entrance into the zero dynamics of the closed loop system, resulting in a long time needed for q_p to reach q_{p_d}. This long time is caused by the excitation of the higher modes due to the fast control of the beam. However, controlling q_a slowly resulted in a longer period for q_a. This lead to the conclusion that there should exist a set of gains that would result in a minimal time needed for control.

To find the optimal set of control gains, t_i is plotted for each of the three DOFs as a function of the two control gains, resulting in the 3-D plots as shown in Figure 4.2. Looking at this figure, the behavior that is mentioned before can be noticed. For large gains, q_{a_d} is reached fast while q_{p_d} is reached slowly. Whereas for small gains, q_{a_d} is reached slowly while q_{p_d} is reached shortly after q_{a_d}. The best performance is accomplished with $\lambda = 30$ and $\eta = 30$ ($k_d = 60$ and $k_p = 900$). These gains result in the following end times: $t_{a_{end}} = 1.24$ [sec], $t_{m_{end}} = 1.76$ [sec] and $t_{\xi_{end}} = 1.96$ [sec]. The system behavior of the DOFs during simulations is presented in Figure 4.3.

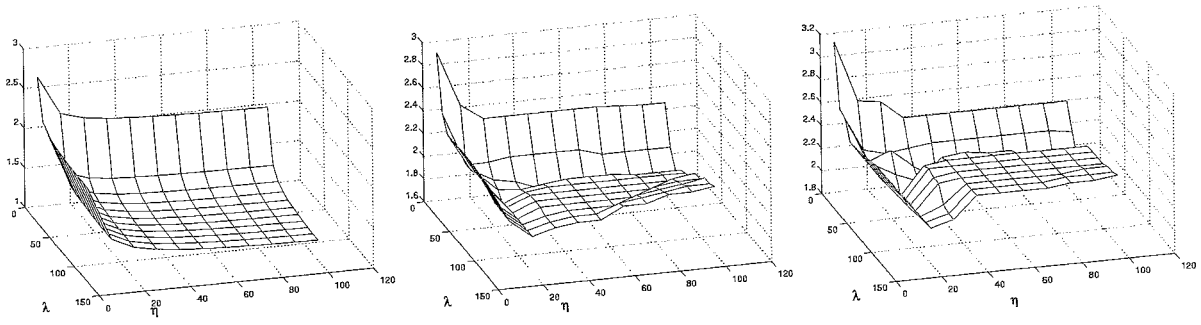

(a) $t_{a_{end}}$ of q_a. (b) $t_{m_{end}}$ of q_m. (c) $t_{\xi_{end}}$ of ξ.

Figure 4.2: The end times t_i.

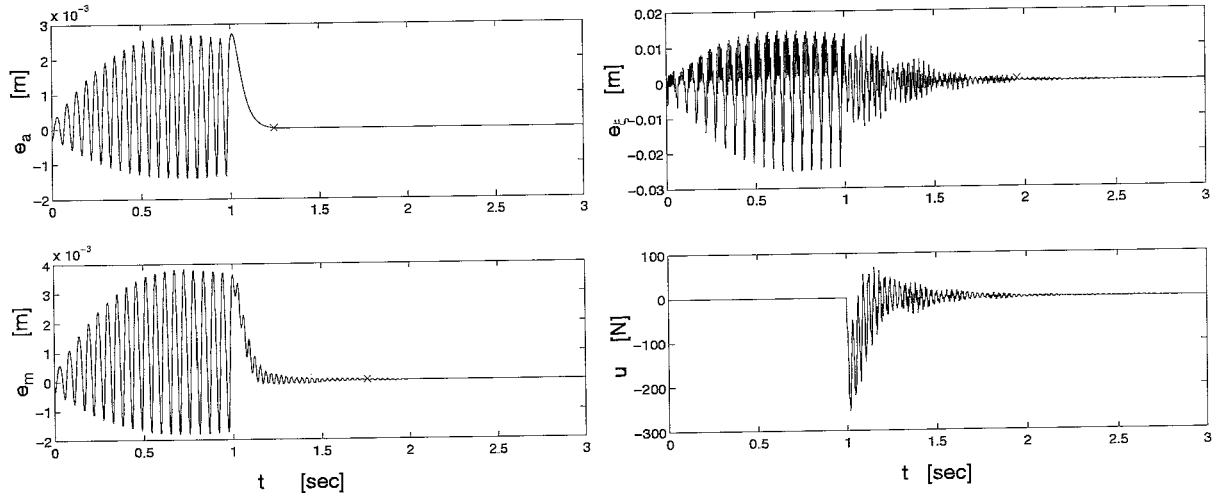

Figure 4.3: The behavior of the nonlinear beam system when controlled using PFL with the optimal set of gains: $k_d = 60$ and $k_p = 900$.

Control of the passive DOFs; the non-collocated case

The first thing that is done in the non-collocated case is checking if the conditions, to make control with PFL possible, are satisfied (see Section 2.2). First, the system has to be locally inertially coupled; as M_{pa} has full rank the condition for coupling is satisfied. Second, the number of q_p has to be less than or equal to the numbers of inputs; as the number of $q_p = 2$ and there is only one input, the second condition is not satisfied and control with PFL is not possible.

Nevertheless, there are some possibilities to make control of q_p possible with PFL. The first option is to use the fact that the two desired trajectories for q_p (q_{m_d} and ξ_d) are not independent. They are both part of the unstable solution of the uncontrolled beam system. The second option is to adapt PFL in such a way that control of a part of q_p becomes possible. For example trying to control q_m instead of both passive DOFs. Both option are not investigated further in this study because it is expected that the system exhibits non-minimum phase behavior when controlling q_m. If the system exhibits non-minimum phase behavior control with PFL is not possible. In Slotine and Li [7], it is showed that non-minimum phase systems cannot be controlled with control methods that achieve perfect or asymptotic convergent tracking. PFL is such a method.

To find out if a system has non-minimum phase behavior the following definition by Slotine and Li [7] for a minimum phase system is used: *The nonlinear system is said to be asymptotically minimum phase if the zero-dynamics is asymptotically stable.* Reversely can be said that a nonlinear system is non-minimum phase if the zero dynamics is unstable. To verify if the beam system is a non-minimum phase system when q_m is controlled, we have to investigate the zero dynamics of the beam system where q_m is considered as the output. This results in the following equation describing the zero dynamics:

$$M_{2\,3,1\,3}\ddot{q}_u + B_{2\,3,1\,3}\dot{q}_u + K_{2\,3,1\,3}q_u = H_{2_{2\,3,1}}F_e. \tag{4.9}$$

The output q_m is assumed to be zero (see the definition of the zero dynamics in Section 2.2) and q_u is represented by the uncontrolled DOFs $[q_a\ \xi]^T$. By the fact that q_m is zero, the force of the one-side spring is zero, resulting in a linear differential equation (4.9) describing the zero dynamics. Assuming that the right side of Eq. (4.9) is zero, the resulting differential equation is unstable; the poles of the remaining linear equation are: 1.6 10^3, -1.5 10^3 and -7.2$\pm$ 3.6 10^2 i. With this knowledge, it is reasonable to assume that Eq. (4.9) is unstable and that the nonlinear beam system is a non-minimum phase system, when controlling q_m.

The fact that the beam system has non-minimum phase behavior when controlling q_m can be made reasonable in another way. It is know that non-minimum phase systems show a typical behavior when a step in the input is applied on the system. The output will move in the opposite direction expected from the input before moving in the expected direction. To see if the beam systems shows this behavior we simulate the behavior of the system with a positive step as input on q_a whereas the behavior of the output q_m is observed. q_m shows the typical behavior of a non-minimum phase system (see Figure 4.4). This non-minimum phase behavior can be understood physically, by the fact that the third eigenmode of the linear beam plays an important role. At the actuator position the influence of this mode is in the opposite direction compared to the influence of this mode at the middle of the beam.

4.4 Simulation with Computed Desired Computed Torque Control

The second control technique that is used to realize vibration reduction for the nonlinear beam system is CDCTC. The model description of the beam system Eq. (4.1) has to be related to the one used with CDCTC, see Eq. (2.26). The system matrices M, B, K are the same for both descriptions, for the values we

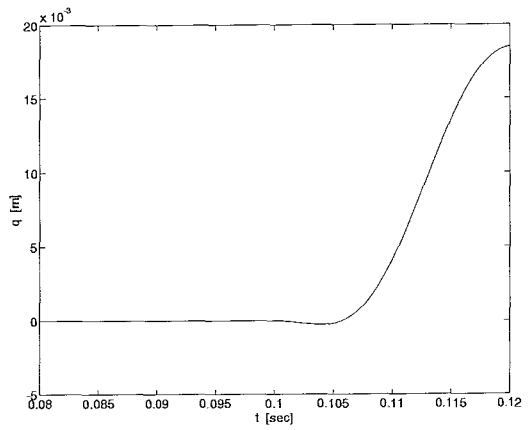

Figure 4.4: The response of q_m when a step in the input is applied on the system.

refer to Appendix A, while $C = 0$ due to the absence of Coriolis and centrifugal forces. For the remaining matrices of CDCTC the following relations are given:

$$f_n = \begin{bmatrix} 0 \\ F_{nl} - F_e \\ 0 \end{bmatrix}, \quad H = H_3 = \begin{bmatrix} 0 \\ 1 \\ 0 \end{bmatrix}, \quad N = \begin{bmatrix} 0 & 0 \\ 1 & 0 \\ 0 & 1 \end{bmatrix}.$$

As in Section 3.4 it is possible to give the equations for computing the input and the pseudo desired trajectories for the uncontrolled DOFs, before deciding which DOF is controlled. This results, using Eq. (2.32) and (2.33), in the following equations:

$$u = M_{1,1:3}\ddot{q}_d + B_{1,1:3}\dot{q}_d + K_{1,1:3}q_d + f_{n_1} + K_{d_{1,1:3}}\dot{e} + K_{p_{1,1:3}}e, \tag{4.10}$$

$$0 = M_{2:3,1:3}\ddot{q}_d + B_{2:3,1:3}\dot{q}_d + K_{2:3,1:3}q_d + f_{n_{2:3}} + K_{d_{2:3,1:3}}\dot{e} + K_{p_{2:3,1:3}}e, \tag{4.11}$$

where K_d and K_p are gain matrices. Eq. (4.10) is used to compute the input and Eq. (4.11) is used to compute the pseudo desired trajectories for the uncontrolled DOFs. These pseudo desired trajectories are not the same as the desired trajectories computed with DIANA that represents the unstable harmonic response. To separate the desired trajectories from the pseudo desired trajectories, the subscript D is used when referred to the pseudo desired trajectories. The division between the controlled and the uncontrolled DOFs is written as:

$$q = L_c\, q_c + L_u\, q_u, \tag{4.12}$$

where the values of L_c and L_u depend on which DOF is controlled. With Eq. (4.12) the column q_d used in Eq. (4.10) and (4.11) is written as:

$$q_d = L_c\, q_{c_d} + L_u\, q_{u_D}. \tag{4.13}$$

Since there is one input, one DOF can be controlled. As there are three DOFs, three cases can be distinguished. In the first case the active DOF q_a is controlled. This case is called, according to PFL, the collocated case. In the second case q_m is chosen as the controlled DOF. Despite the fact that in this case not all passive DOFs are controlled, this case is called, in agreement with PFL, the non-collocated case. In the third case the virtual DOF ξ is chosen as the controlled DOF. However, this case is not investigated in this study because ξ represents no physical DOF, which means that error feedback in practice becomes more difficult due to the fact that ξ cannot be measured. Whether the chosen DOF can be controlled in the three cases depends on the possibility of computing a bounded q_{u_D}.

Control of the actuator DOF; the collocated case

In the collocated case q_a is chosen as the controlled DOF. The values for L_c and L_u can be given as:

$$L_c = \begin{bmatrix} 1 \\ 0 \\ 0 \end{bmatrix}, \quad L_u = \begin{bmatrix} 0 & 0 \\ 1 & 0 \\ 0 & 1 \end{bmatrix}.$$

The first thing to do is to check whether a bounded pseudo desired trajectory for q_u can be computed. Therefore, Eq. (4.11) is written as:

$$\begin{aligned} M_u \ddot{q}_{u_D} + (B_u + K_{d_u})\dot{q}_{u_D} + (K_u + K_{p_u})q_{u_D} = -(M_c \ddot{q}_{c_d} + (B_c + K_{d_c})\dot{q}_{c_d} \\ +(K_c + K_{p_c})q_{c_d} + N^T f_n - K_{d_u}\dot{q}_u - Kd_c\dot{q}_c - K_{p_u}q_u - Kp_c q_c), \end{aligned} \tag{4.14}$$

where:

$$\begin{array}{lllll} M_u = N^T M L_u & B_u = N^T B L_u & K_u = N^T K L_u & K_{d_u} = N^T K_d L_u & K_{p_u} = N^T K_p L_u \\ M_c = N^T M L_c & B_c = N^T B L_c & K_c = N^T K L_c & K_{d_c} = N^T K_d L_c & K_{d_p} = N^T K_p L_c. \end{array}$$

Whether Eq. (4.14) can be used to compute a bounded solution for q_{u_D} depends on the system values. The nonlinear beam matrices result in a stable differential equation for q_{u_D}. This makes it possible to compute bounded pseudo desired trajectories for the passive DOFs and, thus, satisfying the condition for using CDCTC. To make sure that vibration reduction is realized for the entire beam, all DOFs have to become equal to the unstable harmonic response, eventually. This is not possible with CDCTC, it can only be guaranteed that q_u remains bounded. However, CDCTC does guarantee that q_c becomes equal to q_{c_d}. In Section 4.3 is shown that the behavior of q_u can then be described by the zero dynamics of the closed loop system. To make sure that vibration reduction is realized for the whole beam, again it has to be shown that q_{u_d} is a globally asymptotically stable solution of the zero dynamics of the closed loop system.

To find out which control method performs best, PFL or CDCTC, a comparison has to be made for the same simulation conditions. The initial conditions are the values of q and $\dot{q}$ at $t = 1$ [sec]. Furthermore, the initial conditions for q_{u_D} and $\dot{q}_{u_D}$ have to be chosen. As in Section 3.4 these conditions are chosen the same as the initial values for q_u and $\dot{q}_u$ at $t = 1$ [sec]. To quantify the performance of the control methods, the same definition as in Section 4.3 is used. Since we are not interested in the time the system needs to reach the pseudo desired trajectories, the error e^* instead of e is used, because we are interested in the time the system needs to reach the unstable harmonic response; e^* is defined as $e^* = q_d^* - q$ and q_d^* represents the unstable harmonic response.

Trying to find the set of control gains that performs better than PFL, a control gain study has been carried out. Initially, only diagonal gain matrices were used to restrict the number of gains that had to be chosen. The influence of the gains on the performance, however, is very complex because the extra input contribution cannot be predicted. This extra input contribution is a result of the feedback of the uncontrolled DOFs. Carrying out various simulations revealed no possibility to improve the performance compared to that with PFL. Using gain matrices with non-diagonal elements could not change this. An explanation can be given when looking at the error equation of CDCTC:

$$\ddot{e} + M^{-1}(B + K_d)\dot{e} + M^{-1}(K + K_p)e = 0. \tag{4.15}$$

In this equation it can be seen that the feedback of errors is partly determined by the system matrices. This makes the error feedback coupled with the system dynamics which means that it is not possible to go beyond the error reduction determined by the system dynamics. Especially large values of K cause large imaginary parts of poles, or poles that are placed far in the left half plane. To illustrate the coupling of the

feedback with the system dynamics, simulations are presented in Figure 4.5, where the gain matrices are being kept zero. In Figure 4.5b not $e_u = q_{u_D} - q_u$ but $e_u^* = q_{u_d} - q_u$ is displayed, as we are interested in the time when the system reaches the unstable harmonic response.

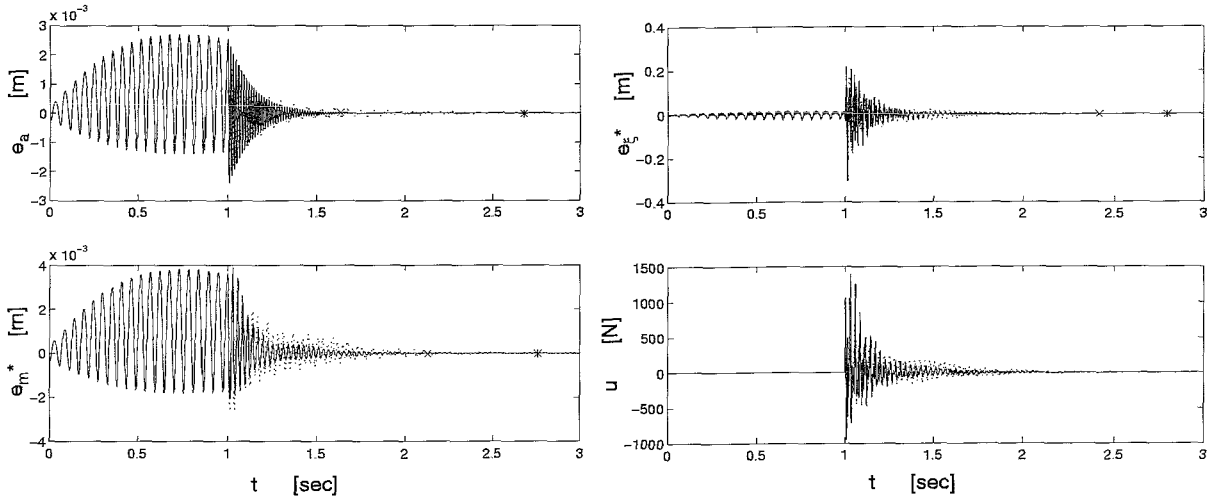

Figure 4.5: Simulations of the beam where the dotted line represents CDCTC ($K_d = 0$, $K_p = 0$) and the end times of CDCTC are marked with x. The solid line represents the behavior with PFL ($k_d = 15$, $k_p = 1.9\ 10^5$) and the end times of PFL are marked with $*$.

To illustrate the influence of the extra input contribution a comparison of simulations with CDCTC and PFL has been made. To do this in a fair way the influence of the feedback of $\dot{e}_a$ and e_a has to be the same for both control techniques. This results in the following relations between the control gains:

$$k_d = (M^{-1}B)_{1,1} + (M^{-1}K_d)_{1,1}, \qquad k_p = (M^{-1}K)_{1,1} + (M^{-1}K_p)_{1,1}. \tag{4.16}$$

When the control gains satisfy Eq. (4.16), the extra input contribution is the only difference between the two control methods. By comparing simulations, it can be seen that the extra input contribution of CDCTC always has a negative influence on the performance. To show this a simulation ($k_d = 15$, $k_p = 1.9\ 10^5$) with PFL together with a simulation ($K_d = 0$, $K_p = 0$) with CDCTC is displayed in Figure 4.5. A lack of explanation for the negative influence of the extra input contribution on the performance is due to the fact that the influence of the gains on this extra input contribution remains unclear. Furthermore, the extra input contribution is determined by the pseudo desired trajectory, which is not related to the unstable harmonic response.

To see if it is possible to realize the same performance with CDCTC as with PFL we change the input. This is done in such a way that the feedback can be chosen without a coupling to the system dynamics. The new input is:

$$Hu = M\ddot{q}_d + B\dot{q} + Kq + K_d\dot{e} + K_p e + f_n, \tag{4.17}$$

where K_d and K_p are constant diagonal gain matrices. This new input results in the following error equation:

$$M\ddot{e} + K_d\dot{e} + K_p e = 0. \tag{4.18}$$

The error equation shows that with this new input the error feedback is no longer determined by the system matrices and can be chosen as desired. This new input will be referred to as CDCTC*. To use CDCTC* in the collocated case it has to be possible to compute a bounded q_{u_D}. To compute q_{u_D}, the passive part of Eq. (4.17) is written as:

$$\begin{aligned} M_u\ddot{q}_{u_D} + K_{d_u}\dot{q}_{u_D} + K_{p_u}q_{u_D} = &-(M_c\ddot{q}_{c_d} + K_{d_c}\dot{q}_{c_d} + K_{p_c}q_{c_d} + N^T f_n \\ &+(B_u - K_{d_u})\dot{q}_u + (B_c - Kd_c)\dot{q}_c + (K_u - K_{p_u})q_u + (K_c - Kp_c)q_c). \end{aligned} \tag{4.19}$$

(4.19) is a stable differential equation for q_{u_D} which makes the on-line computation of a bounded q_{u_D} possible.

As we want to realize the same performance as with PFL, the initial conditions have to be chosen similar. Within the simulations the gain matrices K_d and K_p are chosen as:

$$K_d = M^{-1}\,K_d^*, \qquad K_p = M^{-1}\,K_p^*. \tag{4.20}$$

The error equation can be written as:

$$\ddot{e} + K_d^*\,\dot{e} + K_p^*\,e = 0. \tag{4.21}$$

In the case that the gain matrices are chosen diagonal, the extra input contribution becomes zero, resulting in the same performance as with PFL. In the case that the gain matrices are not diagonal, the extra input contribution has, as with CDCTC, a negative influence on the performance.

Control of the DOF at the middle of the beam; the non-collocated case

The controlled DOF in the non-collocated case is q_m. In Section 4.3 was shown that when q_m is controlled, non-minimum phase behavior occurred. Non-minimum phase behavior makes is impossible to use control methods that achieve prefect or asymptotic convergent tracking errors (Slotine and Li, [7]). CDCTC is a control method that achieves asymptotic convergent tracking errors and, therefore, control with CDCTC in the non-collocated case is not possible.

4.5 Simulation with Computed Reference Computed Torque Control

The third and last technique that is used to control the beam system is CRCTC. The system description used for CRCTC is the same as the one used for CDCTC.

It is possible with CRCTC, just as it is with CDCTC, to give the equations for the computation of the input u and the reference trajectories q_r, before it is clear which DOF is controlled. These equations are given by (See Section 2.4):

$$u = M_{1,1:3}\ddot{q}_r + B_{1,1:3}\dot{q}_r + K_{1,1:3}q_r + f_{n_1} + K_{r_{1,1:3}}\,\dot{e}_r, \tag{4.22}$$

$$0 = M_{2:3,1:3}\ddot{q}_r + B_{2:3,1:3}\dot{q}_r + K_{2:3,1:3}q_r + f_{n_{2:3}} + K_{r_{2:3,1:3}}\,\dot{e}_r, \tag{4.23}$$

where K_r is a gain matrix, and the reference trajectories are defined as:

$$\begin{aligned} \dot{q}_{c_r} &= \dot{q}_{c_d} + \Lambda_c\,e_c, & e_c &= q_{c_d} - q_c, & e_{c_r} &= q_{c_r} - q_c, \\ \dot{q}_{u_r} &= \dot{q}_{u_D} + \Lambda_u\,e_u, & e_u &= q_{u_D} - q_u, & e_{u_r} &= q_{u_r} - q_u. \end{aligned} \tag{4.24}$$

The active part (Eq. (4.22)) is used to compute the input and the passive part (Eq. (4.23)) is used to compute q_{u_r}. In the definition of $\dot{q}_{u_r}$, $\dot{q}_{u_D}$ is used to make a distinction between the pseudo desired trajectory $\dot{q}_{u_D}$ and the unstable harmonic response represented by $\dot{q}_{u_d}$. However, as $\dot{q}_{u_r}$ is computed with Eq. (4.23) the value of $\dot{q}_{u_D}$ remains unknown.

As with CDCTC it is possible to distinguish three cases when selecting the controlled DOF. With CRCTC only the collocated case, where q_a is controlled, is investigated. The two other possible cases are omitted due to different reasons. The case where q_m is controlled is omitted because control with CRCTC is impossible as a result of non-minimum phase behavior (See the non-collocated case in Section 4.3 and 4.4). The case where ξ is controlled is omitted because in practice the displacements and velocities cannot be measured.

Control of the actuator DOF; the collocated case

Using CRCTC in the collocated case means that the active DOF q_a is controlled. This only leads to the desired behavior when it is possible to compute a bounded q_{u_r}. Therefore Eq. (4.23) is written as:

$$\begin{aligned} M_u\ddot{q}_{u_r} + (B_u + K_{r_u})\dot{q}_{u_r} + K_u q_{u_r} = \\ -(M_c\ddot{q}_{c_r} + (B_c + K_{r_c})\dot{q}_{c_r} + K_c q_{c_r} + N^T f_n - K_{r_o} q_u - Kr_c q_c), \end{aligned} \tag{4.25}$$

with:

$$K_{r_u} = N^T K_r L_u \qquad K_{r_c} = N^T K_r L_c.$$

For the remaining system matrices and the values for L_c and L_u the reader is referred to the collocated case of Section 4.4. The system values of the nonlinear beam system together with the control gains result in a stable differential equation for q_{u_r}, which enables the computation of bounded reference trajectories. It is not possible to guarantee that all DOFs will reach the unstable harmonic response. CRCTC only guarantees that q_u remains bounded while q_c reaches q_{c_d}. Again the zero dynamics of the closed loop system describes the system behavior when $q_c = q_{c_d}$. The only way to be sure that all DOFs reach there desired trajectories, is by showing that q_{u_d} is a globally asymptotically stable solution of the zero dynamics of the closed loop system (see Section 4.3).

Simulations with CRCTC are carried out under the same conditions as used earlier with PFL and CDCTC. For CRCTC the initial conditions of q_r and $\dot{q}_{u_r}$ are chosen the same as the corresponding values for q and $\dot{q}_u$ at $t = 1$ [sec]. The control performance is determined with the same definition as used in Section 4.3. Again e^* is used instead of e, where $e^* = q_d^* - q$, and q_d^* is the column that represents the unstable harmonic response of the beam system.

An extensive control gain study has been carried out to find a set of gains that makes CRCTC perform better than PFL. Just like the other two control techniques, the input of CRCTC compensates only for the behavior of q_u on q_c when $q_c = q_{c_d}$. The system behavior is insensitive for changes in the control gains. Furthermore, the little influence that is noticed when changing the gains is very difficult to interpret due to the extra input contribution, caused by the feedback of $\dot{e}_{u_r}$. The best performance that is found with CRCTC is realized with $K_r = 0$ and $\Lambda_c = 10$ and is shown in Figure 4.6. For this set of gains the end times are $t_{a_{end}} = 1.25$ [sec], $t_{m_{end}} = 1.95$ [sec], and $t_{\xi_{end}} = 2.17$ [sec] which are slower than the end times that can be realized with PFL.

To explain the system behavior using CRCTC, the error equation is given as:

$$M\ddot{e}_r + (B + K_r)\dot{e}_r + K e_r = 0. \tag{4.26}$$

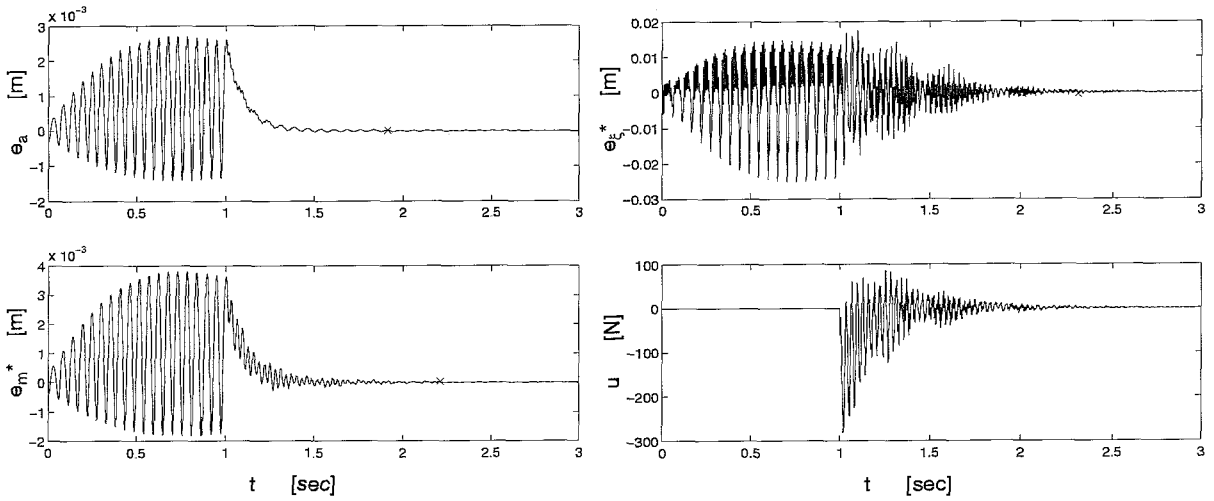

(a) (b)

Figure 4.6: The behavior of the nonlinear beam system when controlled with CRCTC, with the following set of gains: $K_r = 0$ and $\Lambda_c = 10$.

Using the definition for e_r, Eq. (4.26) is written as:

$$M\ddot{e} + (M\Lambda + B + K_r)\dot{e} + ((B + K_r)\Lambda + K)e + K\Lambda \int e = 0. \tag{4.27}$$

This error equation shows that the feedback is partly determined by the system matrices. The feedback, as a result of the system matrices, is a possible explanation for the insensitivity of the performance for changes in the gains. The coupling of error feedback with the system dynamics makes it impossible to go beyond the error reduction determined by the system dynamics. It, however, only partly explains the decreasing performance with CRCTC in relation to PFL.

CRCTC cannot be compared with PFL in a fair way in order to find out what the influence is of the extra input contribution due to the integral action. It remains unclear if the difference in performance is caused by this integral action or by the extra input contribution resulting from the error feedback of the uncontrolled DOFs. The influence of the control gains on the reference trajectories remain unclear, and as the extra input contribution is determined by the reference trajectories the influence of the gains on that contribution remain unclear. Furthermore, the reference trajectories, and so the extra input contribution, are not related to the desired trajectories for the beam.

The input of CRCTC can be adapted in such a way that the integral action disappears from the error equation. Furthermore, the input can be chosen such that there is no longer a coupling between the feedback and the system dynamics. However, this adaptation has not been implemented because, as shown with CDCTC, no knowledge on the influence of the extra input contribution could be gained by doing so.

4.6 Discussion

In this chapter three control methods were used to control the nonlinear beam system. The objective was to realize vibration reduction for the entire beam by controlling one DOF to its unstable harmonic response.

For PFL two cases have been distinguished: control of the active DOF (the collocated case) or control of the passive DOFs (the non-collocated case). In the first case the usefulness of the zero dynamics of the closed loop system has been shown. By proving that the desired trajectories for the uncontrolled DOFs are a globally asymptotically stable solution of the zero dynamics of the closed loop system, vibration reduction for the entire beam could be guaranteed. The total performance was determined by the poles of the error equation of the controlled DOF and the values of the uncontrolled DOFs when entering the zero dynamics of the closed loop system. Control in the second case, the non-collocated case, was not possible because there were more DOFs than inputs.

For CDCTC also two cases have been distinguished. First, the collocated case where the active DOF is controlled. Second, the non-collocated case where the middle of the beam is chosen as controlled DOF. With CDCTC it can only be guaranteed that the uncontrolled DOFs remain bounded. To guarantee that the uncontrolled DOFs approach the unstable harmonic response, this response has to be a globally asymptotically stable solution of the zero dynamics of the closed loop system. In the collocated case no set of gains was found that resulted in better performance compared to PFL. In contrast to the position control of the cart-pole, where the extra input contribution, created by the feedback of the angle errors, influences the behavior in a positive way no positive influence was determined for the beam system. The main reasons are: feedback is partly determined by the system matrices and so by the system dynamics, and the influence of the gains on the extra input contribution remain unclear. Furthermore, the pseudo desired trajectories are not related to the unstable harmonic response of the beam system. Control of the beam in the non-collocated case is not possible with CDCTC. This is a result of non-minimum phase behavior that the beam system exhibits when the DOF in the middle of the beam is controlled.

For CRCTC only the collocated case, where the active DOF is controlled, is considered. Control of the DOF in the middle of the beam is not possible due to non-minimum phase behavior. To guarantee vibration reduction for the entire beam system the zero dynamics of the closed loop system has to be investigated, because CRCTC only guarantees that the uncontrolled DOFs remain bounded. The control performance of the beam system cannot be improved with CRCTC in comparison to PFL. The reason for the disability to improve control performance are the same as given for CDCTC.

Summarizing it can be said that the extra input contribution created by CDCTC and CRCTC in comparison with PFL can influence the system behavior. However, the lack of understanding into the relation between the extra input contribution and the controlled system behavior made it impossible to use the extra input contribution in such a way that it had a positive influence on the controlled system behavior.

Chapter 5

Conclusions and Recommendations

5.1 Conclusions

Three control methods have been presented for the control of underactuated systems, namely: Partial Feedback Linearization (PFL), Computed Desired Computed Torque Control (CDCTC), and Computed Reference Computed Torque Control (CRCTC). CDCTC and CRCTC can be used more generally than PFL because the restrictions for applying CDCTC and CRCTC are less constrained. However, the computational efforts are much higher for CDCTC and CRCTC than for PFL as a result of the computation of the pseudo desired trajectory and the reference trajectory.

When the nonlinear beam system is controlled to realize vibration reduction by stabilizing the unstable harmonic response, the best control performance is realized with PFL. This in contrast to the control of the cart-pole system where CRCTC performs best. There are two main reasons for this difference in the controlled behavior. The first reason is that the feedback of CDCTC/ CRCTC is partly determined by the system matrices, therefore it is not possible to go beyond the error reduction determined by the system dynamics. This is more dominant for the nonlinear beam system as the system values are larger. The second reason is that the influence of the extra contribution to the input with CDCTC/ CRCTC, is not clear due to the difficulty in relating the effects of the gains, the initial conditions, and the pseudo desired or the reference trajectory to the controlled system behavior.

By proving that the desired trajectories of the uncontrolled DOFs are a globally asymptotically stable solution of the zero dynamics of the closed loop system, it can be guaranteed that all DOFs will eventually converge towards the unstable harmonic response, ones the controlled DOF has reached its desired trajectory. This results in a vibration amplitude reduction for the entire beam while reducing control effort simultaneously. Furthermore, the zero dynamics of the closed loop system can be investigated to get insight into the behavior of the uncontrolled DOFs, ones the controlled DOF has reached its desired trajectory.

With CDCTC and CRCTC it is not possible to guarantee that the vibration reduction is realized for all DOFs, because it is only guaranteed that the uncontrolled DOFs remain bounded. However, with the use of the zero dynamics of the closed loop system such a guarantee can be given.

The DOF in the middle of the beam cannot be controlled with methods that achieve perfect or asymptotic convergent tracking. This is a result of the non-minimum phase behavior that occurs when this DOF is controlled in the way that is described in this report.

5.2 Recommendations

Until now PFL only controls the active or the passive DOFs. To gain more freedom in the control design, PFL could be adapted in such a way that an arbitrary combination between active and passive DOFs becomes possible, as long as the number of controlled DOFs is less than or equal to the number of inputs. This would enable the non-collocated case for the 3-DOF beam system , because the passive DOF q_m or ξ could be chosen to be the controlled DOF.

A control technique that uses the behavior of all DOFs has to be developed. This can be realized by changing the entire controlled error system, i.e. by adding damping and stiffness by means of the controller. The addition of stiffness changes the occurrence of nonlinear phenomena at certain frequencies while the addition of damping always has a positive influence in suppressing nonlinear phenomena, however, at the cost of control effort.

Furthermore, investigation into the possibility to implement the unstable harmonic response instead of a pseudo desired or a reference trajectory within the concepts of CDCTC and CRCTC has to be done. This could certainly improve the control performance because in this way knowledge of the desired system behavior is used directly within the control design.

Bibliography

[1] DIANA, *DIANA 6.0 ed*, TNO building and construction research, Delft ,1995.

[2] R.H.B Fey *Steady-state behaviour of reduced dynamic systems with local nonlinearities*, PhD thesis, Eindhoven University of Technology, 1992.

[3] M.F. Heertjes, M.J.G. v/d Molengraft, J.J Kok, R.H.B. Fey, and E.L.B. van de Vorst, *Vibration control of a nonlinear beam system*, D. H. van Campen (ed.), IUTAM Symposium an Interaction between Dynamics and Control in Advanced Mechanical Systems, pp. 135-142, 1997.

[4] I. Lammerts, *Adaptive computed reference computed torque control of flexible manipulators*, PhD thesis, Eindhoven University of Technology, 1993.

[5] A.R. Kant, *Stabiliseren van instabiele periodieke oplossingen van niet-lineaire mechanische systemen, regelstrategieën stabiliteit en regelbaarheid*, WFW-report 95.083 (in Dutch), Eindhoven University of Technology, 1995.

[6] L.T.A. Sanders, *Controlling a beam with one-sided spring: A zero dynamics based approach to actuator positioning*, WFW-report 97.022 (in Dutch), Eindhoven University of Technology, 1997.

[7] J. Slotine en W Li, *Applied nonlinear control*, Prentice Hall, 1991.

[8] M. Spong, *The swing up control problem for the acrobot*, IEEE Control Systems, pp. 19-55, February 1995.

[9] E.L.B. van de Vorst, *Long term dynamics and stabilization of nonlinear mechanical systems*, PhD thesis, Eindhoven University of Technology, 1996

Appendix A

Model matrices

In this appendix the values for the system matrices are given. M is the mass matrix [kg], B the damping matrix $\left[\frac{\mathrm{Ns}}{\mathrm{m}}\right]$and K the stiffness matrix $\left[\frac{\mathrm{N}}{\mathrm{m}}\right]$.

$$M = \begin{bmatrix} 2.4917 & -7.3935\ 10^{-1} & -1.0067\ 10^{-2} \\ -7.3935\ 10^{-1} & 4.7021 & 2.5515\ 10^{-2} \\ -1.0067\ 10^{-2} & 2.5515\ 10^{-2} & 2.7818\ 10^{-4} \end{bmatrix},$$

$$B = \begin{bmatrix} 3.6559\ 10^{1} & -2.187210^{1} & -1.2497\ 10^{-1} \\ -2.1872\ 10^{1} & 2.9214\ 10^{1} & 1.4174\ 10^{-1} \\ -1.2497\ 10^{-1} & 1.4174\ 10^{-1} & 4.3570\ 10^{-3} \end{bmatrix},$$

$$K = \begin{bmatrix} 3.8290\ 10^{5} & -2.5939\ 10^{5} & -8.8920\ 10^{-10} \\ -2.5939\ 10^{5} & 2.1059\ 10^{5} & 4.3181\ 10^{-9} \\ -8.8920\ 10^{-10} & 4.3181\ 10^{-9} & 6.1075\ 10^{1} \end{bmatrix}.$$

Furthermore, the transition matrices H_1 , H_2 and H_3 are given as:

$$H_1 = H_2 \begin{bmatrix} 0 \\ 1 \\ 0 \end{bmatrix}, \quad H_3 = \begin{bmatrix} 1 \\ 0 \\ 0 \end{bmatrix}.$$

For completeness the values of the remaining constants are given:

$$\begin{array}{lll} k_{nl} = & 1.65\ 10^{5} & \left[\frac{\mathrm{N}}{\mathrm{m}}\right], \\ f_e = & 37 & [\mathrm{Hz}], \\ m_e r_e = & 0.984\ 10^{-3} & [\mathrm{kg\,m}]. \end{array}$$

The Fourier coefficients that are used to calculate the desired trajectory for the DOFs, are given as:

$$C = \begin{bmatrix} -8.1875\ 10^{-5} & -1.2086\ 10^{-4} & 7.1974\ 10^{-15} \\ -1.9966\ 10^{-4} & -2.3765\ 10^{-4} & -4.7595\ 10^{-3} \\ 5.7446\ 10^{-6} & 2.3506\ 10^{-6} & 5.1919\ 10^{-4} \\ -3.6939\ 10^{-6} & 2.5900\ 10^{-6} & -6.7768\ 10^{-4} \\ -3.2456\ 10^{-7} & 6.4545\ 10^{-7} & -9.4666\ 10^{-5} \\ -7.9815\ 10^{-8} & 2.5695\ 10^{-7} & -3.1538\ 10^{-5} \\ 4.0062\ 10^{-8} & -1.7511\ 10^{-7} & 1.9710\ 10^{-5} \\ -7.4595\ 10^{-9} & 4.0194\ 10^{-8} & -4.3080\ 10^{-6} \\ -3.9495\ 10^{-9} & 2.4671\ 10^{-8} & -2.5659\ 10^{-6} \\ 4.1021\ 10^{-9} & -2.8659\ 10^{-8} & 2.9203\ 10^{-6} \\ -1.2171\ 10^{-9} & 9.2615\ 10^{-9} & -9.3022\ 10^{-7} \\ 3.4368\ 10^{-6} & 5.4166\ 10^{-6} & -2.7199\ 10^{-5} \\ -2.5355\ 10^{-7} & -2.6000\ 10^{-7} & -1.0019\ 10^{-5} \\ -9.5507\ 10^{-8} & 3.0718\ 10^{-7} & -3.7700\ 10^{-5} \\ 1.0486\ 10^{-7} & -1.6763\ 10^{-7} & 2.7147\ 10^{-5} \\ 1.4640\ 10^{-8} & -3.3549\ 10^{-8} & 4.6428\ 10^{-6} \\ -8.4442\ 10^{-9} & 2.8158\ 10^{-8} & -3.4184\ 10^{-6} \\ 1.8470\ 10^{-9} & -8.0187\ 10^{-9} & 9.0408\ 10^{-7} \\ 8.9210\ 10^{-10} & -4.4542\ 10^{-9} & 4.8554\ 10^{-7} \\ -1.0845\ 10^{-9} & 6.3227\ 10^{-9} & -6.6659\ 10^{-7} \\ 3.6931\ 10^{-10} & -2.4182\ 10^{-9} & 2.4929\ 10^{-7} \end{bmatrix}.$$

The unstable harmonic response is approximated as:

$$q_{d_j} = C_{1,j} + \sum_{i=1}^{n} C_{i+1,j} \cos(2\pi f_e i t) + \sum_{i=1}^{n} C_{i+(n+1),j} \sin(2\pi f_e i t), \quad n = 10.$$